Photochemical hydrogen generation with porphyrin-based systems

Kalliopi Ladomenou[a], Mirco Natali[b,*], Elisabetta Iengo[c], Georgios Charalampidis[a], Franco Scandola[b,**], Athanassios G. Coutsolelos[a,***]

[a] Department of Chemistry, University of Crete, Laboratory of Bioinorganic Chemistry, Voutes Campus, PO Box 2208, Crete 71003, Greece
[b] Department of Chemical and Pharmaceutical Sciences, University of Ferrara, and Inter-University Center for Chemical Conversion of Solar Energy (SOLARCHEM), Via Fossato di Mortara 17-19, 44121 Ferrara, Italy
[c] Department of Chemical and Pharmaceutical Sciences, University of Trieste, Via L. Giorgieri 1, 34127 Trieste, Italy

Contents

ARTICLE INFO

Accepted 1 October 2014

Keywords:
Porphyrins
Metallo-porphyrins
Hydrogen production
Photocatalysis

ABSTRACT

While its main current use is that of a feedstock in the chemical and petrochemical industry, molecular hydrogen can also be considered, in perspective, as an interesting energy carrier to be used in place of conventional fuels, e.g., in devices such as fuel cells. From this viewpoint, of particular interest would be the possibility to generate hydrogen from water splitting using a source of renewable energy such as solar light. This could represent, in principle, an inexhaustible, environmentally friendly energy source. In this review we summarize recent work on photochemical hydrogen evolution carried out with systems based on porphyrins or metalloporphyrins, either as photosensitizers or as catalysts. The systems discussed are varied including different levels of complexity, performance, and mechanistic insight. In general porphyrin molecules appear as a very promising class of photosensitizers for photocatalytic hydrogen production.

Abbreviations: ADT, azadithiolate; bpy, 2,2′-bipyridine; C, concentration; CTAB, cetyltrimethylammonium bromide; DeAC, decylammonium chloride; EDTA, ethylenediaminetetraacetic acid; ET, electron transfer; Fc, ferrocene; GC, glassy carbon; GDH, glucose dehydrogenase; HEC, hydrogen evolving catalyst; HER, hydrogen evolution reaction; IR, infrared; LB, Langmuir–Blodgett; MOF, metal–organic framework; MV^{2+}, methyl viologen dication; NAD^+, oxidized nicotinamide adenine dinucleotide; NADH, hydrogenated nicotinamide adenine dinucleotide; NADPH, reduced nicotinamide adenine dinucleotide phosphate; Nf, Nafion® membrane; NMI, naphthalene monoimide; Nonidet P-40, (octylphenoxy)polyethoxyethanol; P, light-absorbing photosensitizer; PEC, photoelectrochemical cell; Poly(Glu), anionic L-glutamate polypeptide; prod, irreversible oxidation products of SED; PSA, pyrenesulfonic acid; PVA, polyvinyl alcohol; RGO, reduced graphene oxide; SCE, saturated calomel electrode; SDS, sodiumdodecyl sulfate; SED, sacrificial electron donor; TEA, triethylamine; TEOA, triethanolamine; TFA, trifluoroacetic acid; TOF, turnover frequency; TON, turnover number; TPPH, 5,10,15,20-tetrakis(4-(hydroxyl)phenyl)porphyrin; Triton N-101, polyethylene glycol nonylphenyl ether; Triton X-100, polyethylene glycol p-(1,1,3,3-tetramethylbutyl)- phenyl ether; Tween-40, polyoxyethylenesorbitan monopalmitate; UV–vis, Ultraviolet–visible; WOC, water oxidation catalyst; ZnTPP, zinc tetraphenylporphyrin; Φ, quantum yield; Φ_{H_2}, quantum yield of hydrogen production; Φ_T, quantum yield for formation of the excited triplet state.

* Corresponding author. Tel.: +39 3476039861.
** Corresponding author. Tel.: +39 3404775278.
*** Corresponding author. Tel.: +30 2810545045.
E-mail addresses: mirco.natali@unife.it (M. Natali), eiengo@units.it (E. Iengo), snf@unife.it (F. Scandola), coutsole@uoc.gr (A.G. Coutsolelos).

"Yes, my friends, I believe that water will one day be employed as fuel, that hydrogen and oxygen which constitute it, used singly or together, will furnish an inexhaustible source of heat and light, of an intensity of which coal is not capable. . .. Water will be the coal of the future"
Jules Verne, *L'Ile Misterieuse* (1874)

1. Introduction

The interest in hydrogen as a synthetic fuel began to rise in the 1970s, about one century after the visionary statement by Jules Verne [1–3]. The main original motivation was the concern about depletion of oil reserves, but later on the problem of CO_2 emissions and anthropogenic global warming emerged as an additional, perhaps even more relevant issue. The idea behind the use of hydrogen as an energy carrier [4] is simple: (i) hydrogen is one of the most abundant elements on Earth; (ii) the combustion of molecular hydrogen with oxygen produces heat; (iii) the combination of molecular hydrogen and oxygen in a fuel cell generates electricity and heat; (iv) the only byproduct of such energy-producing processes is water. Therefore, if hydrogen could be produced from water cleanly, using a source of renewable energy, both the energy and the environmental problems of our planet could be solved [5–7]. Among the available renewable energy sources, solar energy is evidently the most attractive one because of its abundance, even distribution, and accessibility (the problem of intermittency is automatically solved by conversion into a fuel). Although hydrogen can in principle be produced by solar energy in an indirect way, i.e., by solar photovoltaics coupled with water electrolysis, direct photoelectrochemical conversion of solar energy into hydrogen by water splitting ("artificial photosynthesis"), though challenging, is by far more attractive.

A simplified scheme with the minimum set [8] of components required for photochemical water splitting is shown in Fig. 1a. The first essential component is a light-absorbing chromophore, usually called photosensizer (P). The excited state, with its high-energy electron and low-energy hole, can accomplish water splitting in either of two ways, water reduction followed by water oxidation or vice versa. Water splitting being endoergonic by 1.23 eV, many dyes absorbing visible light (1.5–3.1 eV) have, in principle, the thermodynamic power to perform this photochemical reaction [9]. The main problems to be faced, however, are of kinetic nature and pertain to the fact that, while the charge separation (and recombination) steps initiated by light absorption are fast one-electron processes, oxidation and reduction of water are intrinsically slow, multi-electron processes. Therefore, essential additional components of any water splitting photochemical cycle are multi-electron catalysts, able to store electrons or positive charges produced by the photosystem and to deliver them to the substrate in low activation energy processes. A large amount of research activity is currently being devoted to the development of efficient water oxidation (WOC) [10] and hydrogen evolving (HEC) catalysts [11–14].

Since the entire water splitting process is complex, with the efficiency limited by several possible shortcuts and charge recombination processes, a convenient strategy to facilitate the study and optimization of sensitizer and catalysts is to isolate one of the half-reactions by providing the charges required on the opposite side with a sacrificial redox agent, i.e., a species that following electron transfer undergoes some rapid reaction making the whole process irreversible. A half-cycle of this kind for the hydrogen generating reaction is shown in Fig. 1b. Convenient sacrificial electron donors (SED), frequently used in this type of experiment, are aliphatic amines, thiols, and ascorbic acid. Analogous schemes for the water oxidation reaction can be easily conceived, using sacrificial electron acceptors (SEA) (as, e.g., persulfate or Co(II) amine complexes).

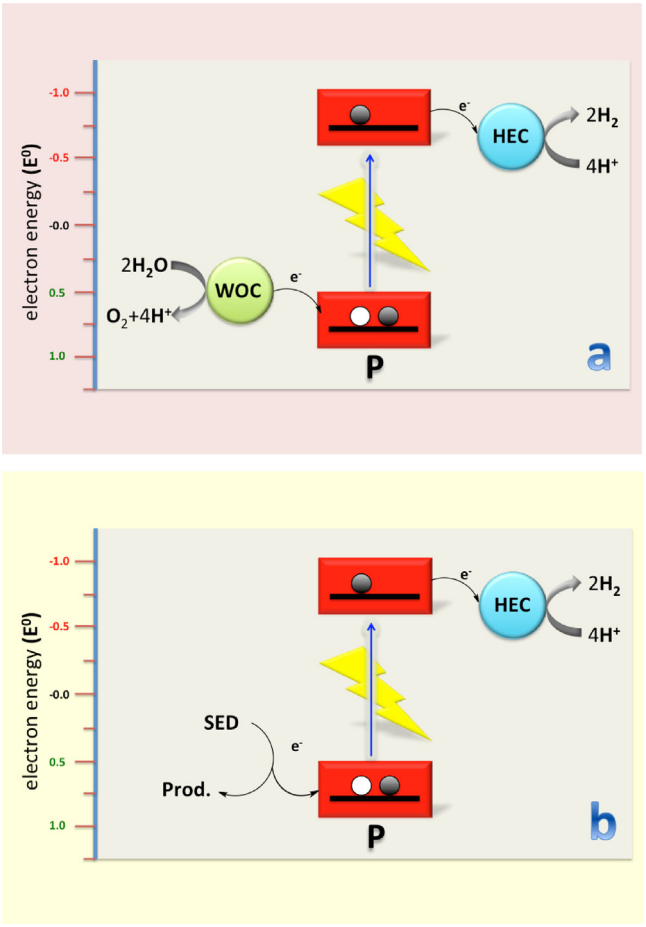

Fig. 1. (a) Simplified scheme for a photochemical water splitting system: P = light-absorbing photosensitizer, WOC = water oxidation catalyst, HEC = hydrogen evolving catalyst; (b) sacrificial half-cycle for photochemical hydrogen evolution: SED = sacrificial electron donor, prod = irreversible oxidation products of SED.

In principle, once each side is optimized in sacrificial cycles, the two half reactions should be combined together in a regenerative system. Among possible coupling strategies, heterogenization onto electrodes and assembling of the full system as a photoelectrochemical cell (PEC) seems to be the most promising one [15–17].

As far as the hydrogen evolving catalysts are concerned, both heterogeneous and homogeneous systems have been used [18]. The most widely used heterogeneous HEC has been, somewhat obviously, platinum metal, usually in the form of colloidal particles in solution [19–22] or supported on various types of materials [23,24]. As alternative heterogeneous HECs, not containing noble metals and thus more suitable for application, NiMoZn alloys [25] as well as Mo and W sulfides [26,27] have also been considered. As to molecular HECs for use in homogeneous solution, a substantial amount of work has been performed using dithiolate bridged di-iron complexes, a class of catalysts inspired by the structure and function of [2Fe2S] natural hydrogenases [28–30]. Along with some Ni phosphine complexes [31], the other main class of molecular catalysts used in photochemical hydrogen evolution studies has been that of macrocyclic cobalt complexes, with molecules of the cobaloxime type playing by far the major role [32–35]. Notably, some work has also been performed using cobalt porphyrins and related structures as HECs (vide infra).

As far as photosensitizers for hydrogen evolution are concerned, both inorganic and organic dyes have been widely used. Among the inorganic species Ru(II) polypyridine complexes, with the prototype $Ru(bpy)_3^{2+}$ [36], have played by far the major role, although

other metal polypyridine complexes (e.g., of Re(I) [37], Ir(III) [38], Pt(II) [39]) have been used as well. Though widely employed for mechanistic studies, most of these systems are noble-metal containing [40], a drawback toward possible applications. On the other hand, a variety of organic dyes have been used as sensitizers in cycles of the type of Fig. 1b, particularly by Eisenberg [41,42]. They have the advantage of being relatively inexpensive, although they may be less stable than the inorganic dyes under hydrogen generating conditions. Moreover, usually working through their long-lived triplet states, they make relatively poor use of the absorbed light energy, a substantial amount of which is lost in singlet-triplet intersystem crossing.

Because of their similarity to the key dyes of natural photosynthesis, porphyrins and metal porphyrins have been extensively investigated from the viewpoint of photoinduced electron transfer processes, both at the molecular and supramolecular level [43–45]. Somewhat surprisingly, however, after some early attempts [46–48], these chromophores have found comparatively little use as organic photosensitizers in photocatalytic water splitting studies. The reasons may partly lie in their limited solubility in aqueous media and in their non-optimal redox properties, especially from the viewpoint of water oxidation. Nevertheless, a new surge of interest in the use of porphyrin based systems for photochemical hydrogen evolution is recently being observed.

In this review we would like to summarize recent work on photochemical hydrogen evolution carried out with systems based on porphyrins or metal porphyrins, either as photosensitizers or as catalysts.

2. Porphyrins as photosensitizers

A large number of photocatalytic hydrogen-evolution systems have been developed since late 1970s. Such systems usually consist of a sacrificial electron donor (SED), a photosensitizer (P), and a hydrogen evolving catalyst (HEC). In some cases, intermediate electron acceptors (EA) may operate as mediators between the photosensitizer and the HEC. In an oxidative cycle the excited state of the chromophore (P*) donates one electron to the catalyst (or the intermediate EA) and the oxidized form of P is reduced subsequently by a SED. In a reductive quenching mechanism, the excited state of the chromophore (P*) abstracts one electron from the SED and the reduced form of the chromophore donates one electron to the catalyst (or the intermediate EA).

The use of the appropriate photosensitizer is very important in order to produce efficient systems. It is necessary that the sensitizer absorbs a considerable fraction of the incident sunlight, throughout the visible region and preferably into the near IR. Moreover, the photosensitizer should have a good stability upon prolonged storage in aqueous solution, no side photoreaction, and an efficient production of separated ion products upon irradiation in the presence of an electron donor or acceptor. In many cases, when the excited-state electron transfer processes are bimolecular, an important requisite of the photosensitizer is that of having a high triplet yield. Porphyrins possess most of the above desired properties in order to be used as photosensitizes for the photoinduced generation of H_2, from a sacrificial system. Moreover, there are numerous reports of facile synthesis of water soluble porphyrins (free base or metalated), that can be prepared by sulphonation, carboxylation or by alkylation of *N*-pyridyl compounds [49].

The absorption spectra of many free base porphyrins have been described in detail [50]. The fairly weak bands in the visible region are normally termed Q bands, whilst the most intense band in the absorption spectrum is the Soret band which is the origin of the second singlet excited state and normally occurs at about 420 nm. The Q region of the absorption spectrum for a metalloporphyrin often consists of two bands, the lowest energy band being the origin of the first excited singlet state, whilst the second band is the vibrational overtone of this latter state. Most of the research for the use of artificial sensitizers involves the synthesis of Zn(II) porphyrins, for which the fraction of the solar spectrum that can be collected is in the order of 30% [51]. Among the various metalated porphyrins the ones containing a metal center among Mg(II), Zn(II), Pd(II), Cd(II), Pt(II), Al(III) or Sn(IV) have the appropriate excited-state properties and stability required for H_2 production systems. Moreover, appropriate substitution at the periphery of the porphyrin ring can be used to fine tune the redox potentials of the porphyrins.

In this section we present porphyrin based photosensitizers combined with diverse catalysts, such as platinum, hydrogenases and cobalt complexes.

2.1. Porphyrins as sensitizers with platinum as catalyst

As discussed in the introduction part, the most widely used heterogeneous HEC is platinum, usually in the form of colloidal particles, but there are also reports of platinum supported on different materials. In this section, various examples regarding the use of porphyrins as photosensitizers and platinum as hydrogen evolving catalyst will be discussed.

2.1.1. Platinum as colloidal particles in solution

Harriman studied various metalloporphyrins as photosensitizers. Hydrogen was formed by irradiation of the porphyrin in aqueous solution containing a series of electron donors (ethanol, glucose, lactate, H_2S, hydrogenated nicotinamide adenine dinucleotide (NADH), carboxylic acids or hydroxylamine) and colloidal platinum [48]. The process obeys a reductive quenching mechanism at the porphyrin triplet level. The efficiency of hydrogen production depends markedly on the type of donor used, with NADH being particularly effective.

In different studies, colloidal platinum has been used as hydrogen evolving catalyst from glucose [52–54]. Also, hydrogen production from glucose with a combination of glucose dehydrogenase (GDH) and hydrogenase has also been reported [55,56]. Saiki and Amao studied a bio hydrogen production system that couples a polysaccharide (sucrose or maltose) degradation with invertase and GDH [57]. Hydrogen produced with colloidal platinum using the photosensitization of the water-soluble zinc *meso*-tetrakis (*p*-sulfonatophenyl) porphyrin (**1**) (Fig. 2) in the presence of methylviologen (MV^{2+}) as an electron relay reagent. Continuous hydrogen gas production was observed when the sample solution containing the polysaccharide, invertase, GDH, nicotinamide adenine dinucleotide (NAD^+), **1**, MV^{2+}, and colloidal platinum was irradiated by visible light. After 240 min irradiation, the amount of hydrogen produced in the system using sucrose or maltose was estimated to be 3.1 or 0.35 μmol, respectively.

Harada and coworkers utilized a complex between a monoclonal antibody for free base and zinc porphyrin in order to construct an energy conversion system [58]. Monoclonal antibody 2B6 was bound to the zinc *meso*-tetrakis (4-carboxyphenyl) porphyrin (**2**) (Fig. 2) and upon binding the lifetime of the excited triplet state of **2** increased from 0.5 to 1.2 ms. A stable cationic radical of viologen was obtained by irradiating a solution containing the complex of 2B6 with **2**, MV^{2+}, and ethylene diamine tetraacetic acid (EDTA). When colloidal platinum was added as a catalyst, photoinduced hydrogen production was observed upon continuous irradiation with visible light. The estimated turnover frequency of photoinduced hydrogen evolution was $5.0 \times 10^{-3}\ s^{-1}$. The heavy chain of antibody 2B6 mainly contributed to the complex formation with **2** and led to the efficient hydrogen production. The amount of hydrogen produced in the presence of antibody 2B6 was eight times larger than that without antibody.

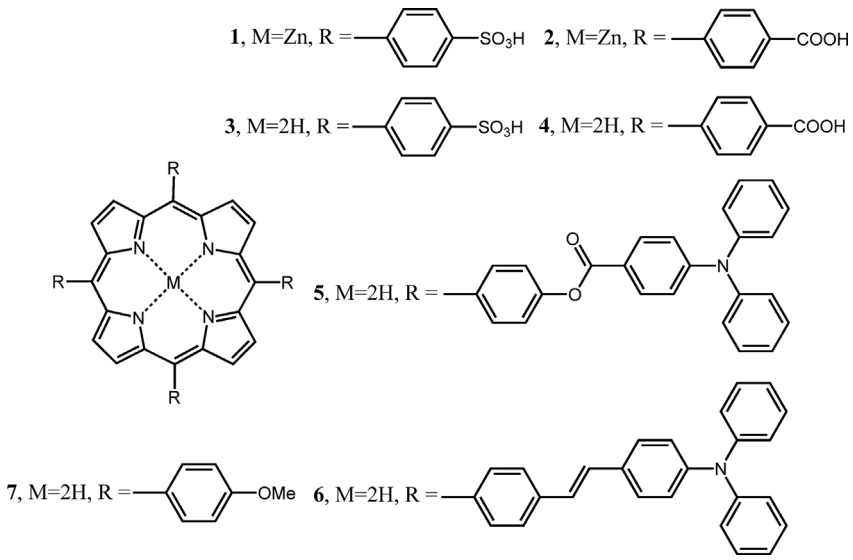

Fig. 2. Molecular structures of porphyrins **1**–**7**.

In another approach, nanocomposites were used as photocatalysts for hydrogen production. These nanocomposites were composed of a *meso*-tetrakis (*p*-sulfonatophenyl) porphyrin (**3**) (Fig. 2) as photosensitizer and platinum (Pt) nanoparticles as catalyst [59]. The porphyrin was also useful in order to prevent agglomeration of the Pt nanoparticles. Fluorescence and photoelectrochemistry studies on **3** and Pt nanocomposites showed that efficient electron transfer occurred from the **3** donor to the metallic nanocore acceptor. Moreover, these nanocomposites were photocatalytically active and produced hydrogen. The turnover numbers (TON_{Pt} and $TON_{\mathbf{3}}$) and quantum yield of hydrogen production (Φ_{H_2}) were 44, 11,056, and 1.8%, respectively, calculated on the basis of the total amount of H_2 evolution after 12 h irradiation.

Rosseinsky and coworkers reported on a water stable porous porphyrin metal–organic framework (MOF), that can perform hydrogen generation from water photocatalytically [60]. The microcrystalline porous material was formed by reaction of $AlCl_3{\cdot}6H_2O$ with the free-base *meso*-tetra (4-carboxyl-phenyl) porphyrin (**4**) (Fig. 2). The zinc derivative (**2**) was also synthesized and the MOF/MV^{2+}/EDTA/Pt system was studied (Fig. 3). For both frameworks a small amount of H_2 was observed after illumination with visible light in the aqueous EDTA/MV^{2+}/colloidal Pt solution for 15 h (quantum yield estimated to be less than 0.01%). Such a low activity was explained on the basis of the diffusion limitations of methyl viologen in the pores. The analogous system in the absence of MV^{2+} gives more efficient hydrogen generation, by a reductive quenching mechanism.

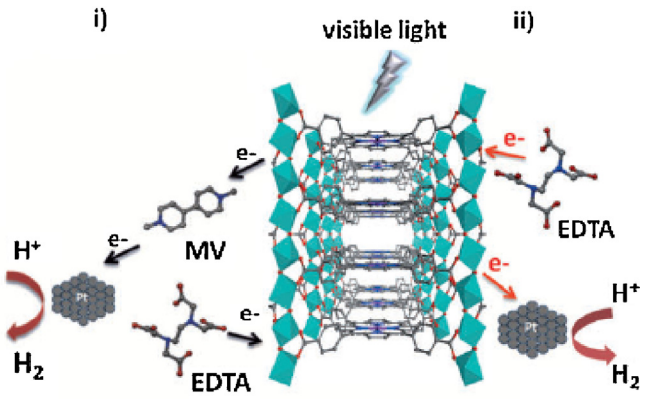

Fig. 3. (i) Reaction involving porphyrin **2**, methyl viologen, colloidal platinum, and sacrificial EDTA. (ii) Reaction involving porphyrin **2**, colloidal platinum, and sacrificial EDTA. Copyright © 2012 Wiley-VCH Verlag GmbH & Co. KGaA, Weinheim. Reprinted with permission from Ref. [60].

In a different study, nanocomposites formed by functionalization of Pt nanoparticles with multibranched-porphyrin photosensitizers were studied [61]. Donor–bridge–acceptor conjugates **5** and **6** were synthesized (Fig. 2). The triphenylamine branches acted as energy donors in these compounds. The organic sensitizers are in direct contact with the metallic core in the nanocomposites, and the electron transfer between the organic moiety and the platinum particles is considered to be efficient. Hydrogen is detected upon UV–vis irradiation of the nanocomposite systems with TON of 4070 and 6590 (vs. porphyrin) for Pt-**6** and Pt-**5**, respectively. The hydrogen evolution by Pt-**6** is higher than that for Pt-**5**, indicating that the ethylene linkage between the tetraphenylporphyrin and triphenylamine moieties is superior to the ester one.

In order to mimic the photo-induced electron transfer process of the photosynthetic reaction center, donor–acceptor covalently linked systems were developed [62]. Yang and coworkers constructed a photocatalytic system that uses a nanocomposite, made of Pt functionalized with 5,10,15,20-tetrakis (4-(hydroxyl)phenyl) porphyrin (TPPH) (**7**) (Fig. 2) and pyrenesulfonic acid (PSA) self-assembled conjugates (Pt–TPPH–PSA), and EDTA as a sacrificial reductant in the absence of an electron mediator [63]. A system without an electron mediator not only is inherently simpler, but also eliminates back reactions associated with the electron transfer to the mediator [64]. It was found that a photoinduced energy transfer from the photoexcited state of pyrene to the porphyrin occurs, followed by an electron transfer from the excited porphyrin moiety to the platinum catalyst. Efficient photocatalytic hydrogen evolution from the system demonstrates the possibility of constructing a photocatalytic system that uses a Pt nanocomposite functionalized by self-assembled donor/acceptor conjugates. The turnover numbers (TON_{Pt} and $TON_{\mathbf{7}}$) and quantum yields (Φ_{H_2}) for the photoinduced hydrogen production system are 63, 6311, and 2.65%, respectively. Somewhat surprisingly, photochemical hydrogen generation only takes place with UV light absorbed by PSA, while visible light absorbed by TPPH is not productive.

Yang and coworkers reported on the use of an organic-inorganic assembly composed of donor–acceptor (D–A) dye molecules and Pt nanoparticles for photoinducing hydrogen evolution from water

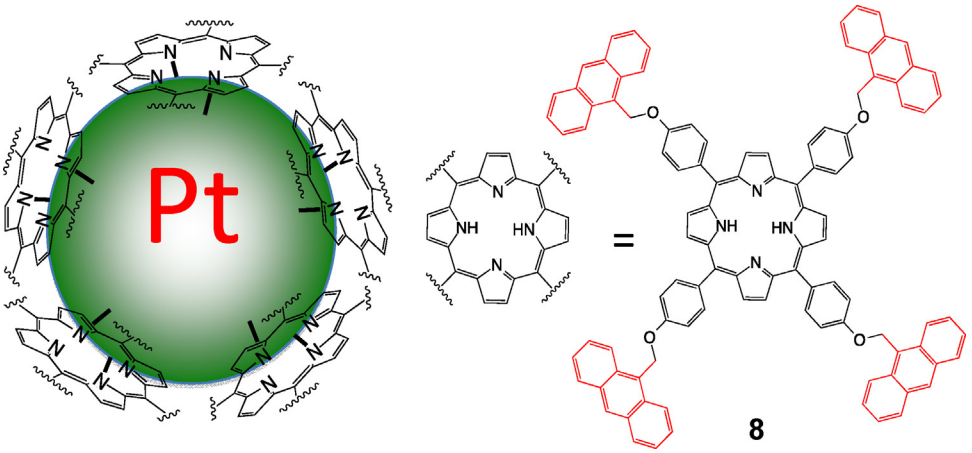

Fig. 4. The proposed configuration of the Pt-**8** nanocomposite [65].

[65]. The dye was porphyrin **8** (Fig. 4) and was functionalized with platinum nanoparticles (Pt-**8**). Interactions among the Pt nanoparticles and the nitrogen atoms of the porphyrin ring are expected and therefore the structure of Pt-**8** can be described as an organic anthryl-porphyrin shell enveloping a Pt metallic nanocore (Fig. 4).

Fluorescence and photoelectrochemical spectra revealed that photoinduced energy transfer occurred from the photoexcited state of anthracene substituents to the porphyrin, followed by an electron transfer from the excited porphyrin moiety to the Pt catalyst. Molecule **8** in the nanocomposite worked as a light-harvesting antenna and the nanocore Pt species acted as a catalyst. The photocatalytic studies showed that after 12 h of UV–vis light irradiation and in the absence of an electron mediator, the total amount of H_2 evolved from the Pt-**8** is 175.3 μmol. In this homogeneous photoinduced hydrogen evolution system, ethanol works as a sacrificial reductant.

2.1.2. *Platinum supported on various materials*

Kalyanasundaram and Grätzel were the first that developed a system with a water-soluble zinc porphyrin (zinc tetramethylpyridyl porphyrin) **9** (Fig. 5) as a photosensitizer, EDTA as the sacrificial donor and Pt as the hydrogen evolving catalyst. This system gave $\Phi_{H_2} = 0.3$, twice the value obtained employing $[Ru(bpy)_3]^{2+}$ as photosensitizer [66]. In this report the platinum catalyst, was supported on polyvinyl alcohol (PVA). In the presence of the optimum concentration of Pt-PVA ($C = 8 \times 10^{-4}$ M) prolonged irradiation of an aqueous solution of **9** (2×10^{-6} M) at pH 5.5 containing EDTA (0.1 M) gave a considerable quantity of hydrogen. The longevity of this system was slightly better than that of the **9**-EDTA-MV^{2+} system [51] (containing methylviologen) so that, although Φ_{H_2} for the **9**-EDTA-MV^{2+} system was higher, the total amounts of hydrogen obtained from exhaustive photolysis were comparable for the two systems. However, the high concentration of platinum required for the **9**-EDTA system is a serious drawback to apply the system in a practical solar energy storing device.

In a following study, water-soluble or insoluble zinc porphyrins (**9**–**12**) were used as sensitizers of platinized TiO_2 for hydrogen production (Fig. 5) [67]. Hydrogen production varies with the concentration of platinum, zinc porphyrin and electron donor on the titanium dioxide surface. Also, the relationship between the rate of hydrogen evolution and pH has a maximum at pH 4–5 for EDTA, ascorbic and oxalic acids, as does the adsorption of these donors on TiO_2. In the case of triethanolamine (TEOA), H_2 production increases sharply in alkaline solutions, in which the TEOA molecules are deprotonated. The photostability of the photosensitizer increases on the semiconductor. Turnover numbers for the zinc porphyrins varied from 50, after 12 h of irradiation for water-soluble zinc porphyrin **9** to up to 150–185, after 9 h of irradiation for water-insoluble sensitizers (**10**–**12**).

In another study the water soluble tin-porphyrin **13** (Fig. 6) was used as a visible light sensitizer of platinized TiO_2 nanoparticles [68]. Hydrogen was successfully produced under visible light irradiation in a wide pH range (pH 3–11). The turnover number of H_2 produced in the SnP/TiO_2 system after 9 h irradiation was 410. The apparent photonic efficiency for H_2 evolution was estimated to be 35% with a monochromatic radiation of 550 nm. The photochemical production of hydrogen is mediated through the formation of the π-radical anion ($SnP^{\bullet -}$) that subsequently transfers electron to TiO_2 in a bimolecular process. The photogenerated $SnP^{\bullet -}$ was monitored by transient absorption spectroscopy and its lifetime is long enough to allow slow diffusion of $SnP^{\bullet -}$ from the bulk solution to the TiO_2 surface, which makes the adsorption of porphyrin **13** on TiO_2 not necessary for hydrogen production.

With the aim of improving the efficiency of electron transfer processes between the porphyrin sensitizer and the redox mediator, viologen-linked porphyrins have been synthesized and

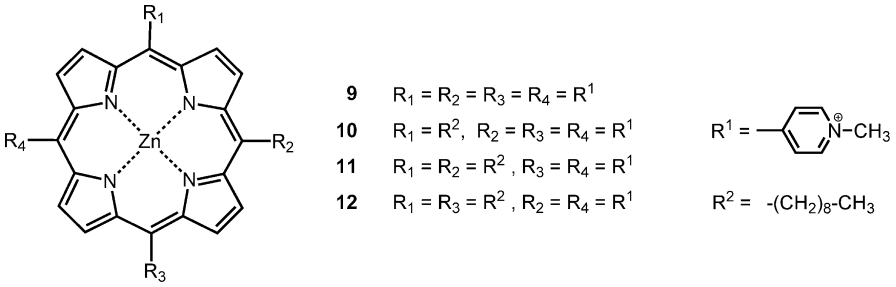

Fig. 5. Molecular structures of porphyrins **9**–**12**.

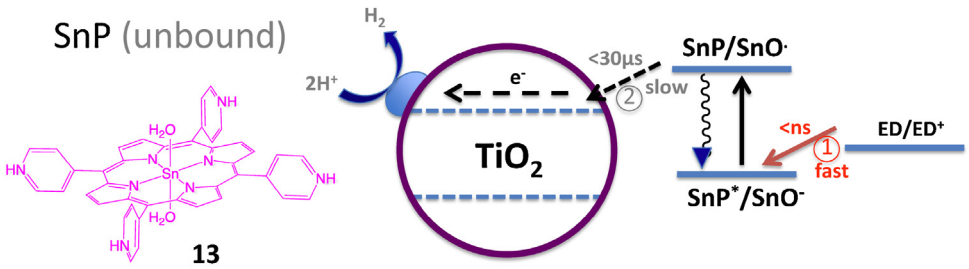

Fig. 6. Schematic illustration of the electron transfer dynamics occurring on SnP porphyrin **13**. Copyright © 2010 Royal Society of Chemistry. Adapted with permission from Ref. [68].

investigated [69–72]. Several studies with respect to photoelectric conversion were reported using electrodes modified with the Langmuir–Blodgett (LB) film of viologen-linked porphyrin to realize a directed electron flow as in the photosynthetic reaction center [73–75]. Negatively charged $PtCl_6^{2-}$ is assumed to be incorporated in the LB films of the positively charged porphyrin moiety and viologen moiety and is reduced to Pt by photoreduction. The Pt particles thus produced are fixed in the LB films. Reduced form of viologen is well-known to be able to reduce protons in the presence of a catalyst such as platinum, leading to H_2 production [51,76–78]. Also, in another study photoreduction of protons to H_2 was observed using a LB film of viologen linked with a free base porphyrin (**14**) (Fig. 7) and in combination with a Pt catalyst in the presence of EDTA as a sacrificial electron donor [79,80]. The rate of hydrogen production using viologen-linked porphyrin **14** was larger than that measured using viologen-free porphyrin **15**. Also, using porphyrin **14**, as compared to porphyrin **15**, hydrogen evolution was continued for a much longer period.

A system using zinc tetraphenyl porphyrin (ZnTPP) (**16**) (Fig. 8) incorporated into a Nafion® membrane (Nf) coated on a platinum electrode (denoted as Pt/Nf[ZnTPP]) produced H_2 [81]. When visible light ($\lambda > 390$ nm) was irradiated on the Pt/Nf[ZnTPP] system, a photocurrent was generated under applied potentials below −0.10 V (vs. Ag/AgCl). The amount of H_2 produced increased with the cathodic potential. These results indicated that in the photochemical primary process, a reductive quenching takes place by electron injection from the Pt electrode to the singlet excited state of ZnTPP forming $ZnTPP^{\bullet -}$, subsequently leading to the H_2 formation by a bimolecular catalysis of porphyrin **16** [81].

Kusumoto and coworkers, reported on the hydrogen production with the insoluble cobalt porphyrin **17** (Fig. 8), MV^{2+}, EDTA and platinum colloid that was loaded on an anionic polypeptide such as the poly(L-glutamate) (Poly(Glu)) [82]. This polypeptide stabilizes the platinum colloid and interacts electrostatically with a cationic decylammonium chloride surfactant (DeAC) to form a polypeptide–surfactant complex. Porphyrin **17** is then solubilized in the polypeptide-complex solution by the hydrophobic interaction with the alkyl chains of DeAC. Hydrogen production experiments carried out in the absence of **17** led to no hydrogen production while at low DeAC concentrations only a trace amount of hydrogen gas was produced. Porphyrin **17** in the Poly(Glu)–DeAC complex can serve as a photosensitizer for the production of hydrogen and the presence of polypeptide–surfactant complexes enhances the rate of this production by solubilizing the photosensitizer and possibly enhancing the separation of charged species. As a general comment, however, the use of cobalt porphyrins as photosensitizers should be regarded with some caution, given the extremely short (ps) excited states lifetimes.

In another study Yang and coworkers prepared an efficient hydrogen evolution system composed of a porphyrin dye functionalized onto Pt nanoparticles as catalyst, and deposited on graphene nanosheets [83]. Porphyrin **7** was used for the noncovalent functionalization of the reduced graphene oxide (RGO), forming the nanocomposite (TPPH–RGO). Compared with either bare **7** or RGO functional Pt nanoparticles, the TPPH-sensitized RGO loaded with Pt nanoparticles shows enhanced photocatalytic activity under UV–vis light irradiation in the presence of TEOA as sacrificial electron donor. The superior electron-accepting and electron transporting properties of graphene greatly accelerate the electron transfer from excited **7** to the Pt nanoparticles, which promote the photocatalytic hydrogen evolution. The authors proposed a possible mechanism for light-driven water reduction by this graphene based nanohybrid with the assistance of CTAB (Fig. 9). (1) Under UV–vis light irradiation, porphyrin **7** molecules adsorbed on RGO sheets are excited, and a photoinduced electron transfer from the **7** moiety to RGO takes place; (2) the electrons are then

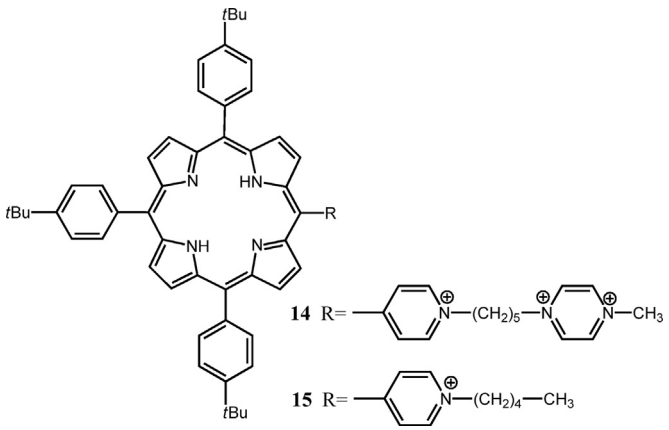

Fig. 7. Molecular structures of porphyrins **14** and **15**.

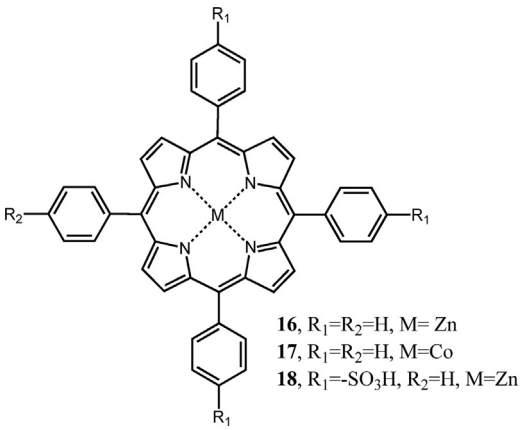

Fig. 8. Molecular structures of porphyrins **16**, **17**, and **18**.

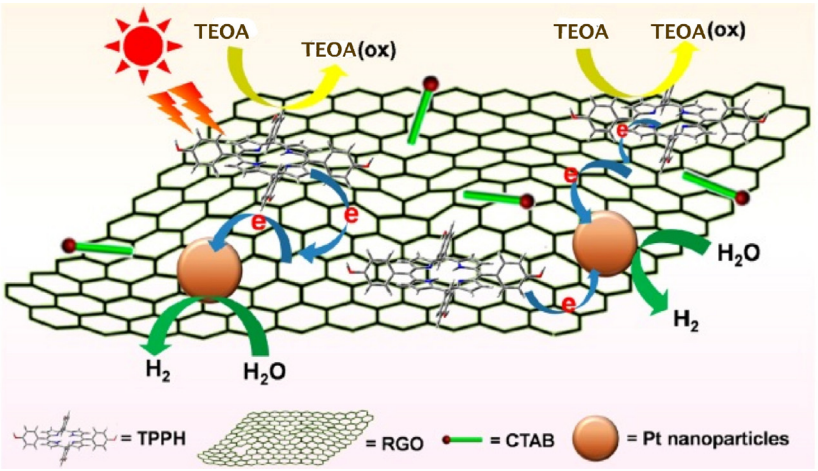

Fig. 9. Schematic photoexcited electron transfer and hydrogen evolution over the RGO–TPPH photocatalyst with the assistance of the CTAB under light irradiation. Copyright © 2013 American Chemical Society.
Reprinted with permission from Ref. [83].

transferred from RGO to the Pt nanoparticles loaded on the graphene nanosheets, where protons are converted into H_2; (3) the oxidized **7** moiety returns back to the ground state by accepting electrons from TEOA. Moreover, with the assistance of cetyltrimethyl ammonium bromide (CTAB) surfactant, the catalytic activity and stability is further improved owing to the prevented aggregation of the TPPH–RGO nanocomposites.

2.2. Porphyrins as sensitizers with Hydrogenase as catalyst

Hydrogenases are enzymes expressed by microorganisms that catalyze the reversible reaction $2H^+ + 2e^- \leftrightarrows H_2$ [84]. They are iron-containing metalloproteins that can be divided in three main classes: the iron–sulfur cluster free hydrogenases, which feature a mono-iron catalytic site; the [NiFe]-hydrogenases, characterized by the presence of a catalytically relevant nickel atom; and the [FeFe]-hydrogenases, which feature the highest catalytic efficiency among the three classes so far characterized and which are generally referred to as the H-cluster [85]. The H-cluster (Fig. 10) consists of a di-iron assembly, the di-iron sub-site [2Fe]H, which is connected to a Fe_4S_4 cluster via a cysteinyl bridge. The cubic Fe_4S_4 cluster is part of the electron transfer chain that links the active site of [FeFe]-hydrogenase. The coordination sphere of the iron centers of the [2Fe]H sub-site is completed by terminal diatomic ligands CO and CN, and by a dithiolate bridge.

Iron hydrogenases are very efficient in reducing protons to molecular hydrogen with turnover frequencies of 6000–9000 molecules H_2 per second per site [86]. In this section the use of the natural enzyme as catalyst will be discussed as well as the study of artificial systems synthesized in order to mimic the active site of the enzyme.

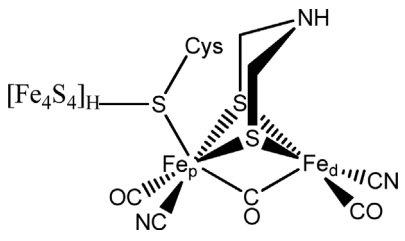

Fig. 10. Schematic structure of the H-cluster found in the active site of [FeFe]-hydrogenases.

2.2.1. Porphyrins as sensitizers using natural enzyme as catalyst

Numerous photoinduced hydrogen evolution systems were developed, in which hydrogenases are used as catalysts [87]. Porphyrins and methylviologen have been widely used as photosensitizers and electron carrier, respectively in these systems [88]. Okura and Kim-Thuan reported a system containing porphyrin **16** (Fig. 7), methyl viologen, hydrogenase from *Desulfovibrio vulgaris* (Miyazaki type) and TEOA or mercaptoethanol as electron donor [89]. Compound **16** being insoluble in water, a micellar solution in an aqueous system was prepared with the aid of a surfactant (Triton X-100). After 15 h of irradiation hydrogen production was observed with a turnover number of 81. In order to avoid the use of surfactants Okura and coworkers synthesized the water soluble porphyrin (**18**) (Fig. 7) and they studied its catalytic activity [90]. Under identical experimental conditions, **18** exhibited superior performance compared to **16** reaching a turnover number of 614. The higher catalytic activity was attributed to the more efficient reduction of MV^{2+} by **18**. Haematoporphyrin was also tested as photosensitizer in a similar photocatalytic system and hydrogen production was observed after visible light irradiation [78].

Cytochrome c_3 is a natural electron carrier and the most suitable substrate for hydrogenase, for this reason it was tested as electron carrier in a photoinduced hydrogen evolution system [91]. When an aqueous solution containing **18**, cytochrome c_3 and TEOA as a reducing agent was irradiated, the absorption spectrum of cytochrome c_3 changed. The Soret band shifted from 419 to 432 nm and this was attributed to the formation of the reduced form of cytochrome c_3. When hydrogenase was added to this system and the mixture irradiated with sunlight for 6 h, hydrogen evolution was observed.

In a different approach viologen-linked zinc porphyrin complexes have been prepared (Fig. 11) [92,93]. The synthesized water-soluble viologen-linked cationic (**19**–**23**) and anionic (**24**–**27**) porphyrins possess different methylene chains between the central macrocycle and the peripheral viologen moieties.

These compounds can act both as photosensitizers and as electron carriers. They were used in combination with reduced nicotinamide–adenine dinucleotide phosphate (NADPH) as electron donor and hydrogenase as catalyst. From fluorescence lifetime measurements and laser flash photolysis experiments it was found that in viologen-linked porphyrins, the photoexcited singlet state and the triplet state of porphyrin are easily quenched by the bonded viologen, compared to the viologen-free porphyrin. When the

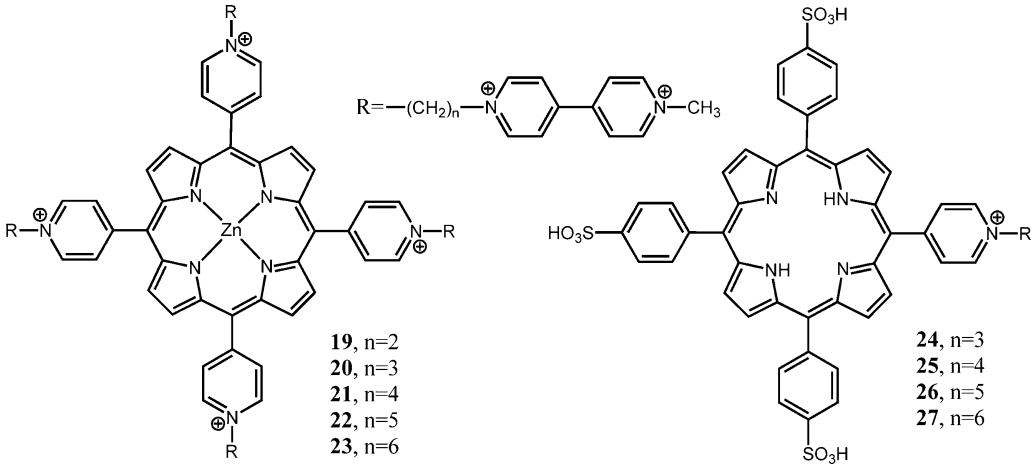

Fig. 11. Molecular structures of viologen linked cationic (**19**–**23**) and anionic (**24**–**27**) porphyrins.

sample solution containing NADPH, porphyrins **19**–**27**, and hydrogenase was irradiated, hydrogen evolution was observed. Within a certain range (n = 2–4), the hydrogen evolution rate decreases with increasing the chain length. In the cases of **22** and **23** however, a higher hydrogen evolution rate was observed [92]. On the other hand with anionic porphyrins (with exception of porphyrin **27**), no hydrogen production was observed.

In order to suppress the back electron transfer from viologen to the porphyrin, micellar systems of surfactant were used [94]. Based on this approach Okura and coworkers reported on a system consisting of TEOA, porphyrin **1**, MV^{2+}, and hydrogenase [95]. Addition of an anionic surfactant, sodium dodecyl sulfate (SDS), resulted in the formation of a SDS micellar system. Although effective charge separation was observed, little hydrogen production was detected because of the denaturation of hydrogenase by SDS. In order to improve the catalytic performance of this system hydrogen evolution was examined in the presence of various non-ionic surfactants (Triton X-100, Nonidet P-40, Triton N-101, and Tween-40) micellar systems [96]. The effective photoreduction of methylviologen and the effective hydrogen production with hydrogenase was observed in the presence of these non-ionic surfactants. In all the cases, the hydrogen production rate was higher compared to that in the absence of the surfactants. The most effective hydrogen production system was developed using Tween-40 micelles. Moreover, the photoinduced hydrogen production rate depends on the alkyl chain length of the surfactant. In a similar catalytic system, the influence on hydrogen evolution of a cationic surfactant, cetyltrimethyl ammonium bromide (CTAB), was also examined [97–99]. The catalytic performance in the presence of this cationic surfactant was superior compared to the anionic and non-ionic surfactants. The increased efficiency was attributed to the more effective suppression of the back electron transfer reaction from reduced methyl viologen to **1**.

Since nature uses multiple chromophoric assemblies (light-harvesting complexes) to capture sunlight and efficiently transfer the energy to the photosynthetic reaction centers, much interest has also been paid to the synthesis of multiporphyrin arrays and organized ultrathin films [100,101]. A very useful and easily controllable technique for the preparation of organized thin films is the LB method, by which many porphyrin organized multilayers have been prepared [102,103]. Qian and coworkers used this method and developed a system in which mixed monolayers of negatively charged phospholipid and positively charged porphyrin **9** were formed at the air–water interface and then transferred onto a glass surface [104]. Both the phospholipid-porphyrin LB films and the porphyrin aqueous solutions were used as photosensitizer for the photoinduced hydrogen evolution, in combination with EDTA, viologen and hydrogenase. Hydrogen production was observed in both cases.

In natural enzymes lysine plays an important role in the effective binding of cytochrome c_3, therefore, in a biomimetic approach, lysine-linked viologen was prepared ($LysV^{2+}$) and applied in a photoinduced hydrogen evolution system containing hydrogenase, porphyrin **4**, and TEOA [105]. Porphyrin **4** was selected as photosensitizer because of the electrostatic repulsion between the four carboxylic groups and the hydrogenase (acidic protein) and thus does not hamper the hydrogenase–LysV complex formation. In this system, under steady state irradiation, efficient hydrogen production was observed. Hydrogen evolution rate with $LysV^{2+}$ was 4 times higher than that with MV^{2+}, indicating that $LysV^{2+}$, which has a high binding affinity for hydrogenase, acts as an effective electron mediator.

Natural hydrogenases are very active hydrogen evolution catalysts. Being prone to chemical and environmental stress, however, enzymes are not suited for long-term use and replacement of hydrogenases with more robust synthetic catalysts, either as homogeneous or heterogeneous species, is most likely the main goal in the field of the HER photocatalysis.

2.2.2. *Porphyrins as sensitizers using biomimetic catalyst*

Iron hydrogenases have received great attention in biomimetic studies aiming at exploring model compounds that can act as proton-reduction catalysts. A few of them have proved to be efficient for electrochemical hydrogen production [106–109]. The photoinduced electron transfer (ET) from a chromophore to a diiron hydrogenase model complex has been observed in a few cases [110,111], but the ultrafast dynamics of this process is still not fully understood. Most of the model compounds that have been used are not covalently linked but are held in suitably close proximity by the protein matrix via non-covalent interactions. On the other hand, several biomimetic [2Fe2S] complexes covalently linked to ruthenium or porphyrin photosensitizers have been synthesized, and the possibility of ET was investigated [112–115].

Song and coworkers studied a model compound **28** in which a photosensitizing porphyrin is covalently linked to the N atom of the diiron azadithiolate (ADT) moiety [$(\mu$-$SCH_2)_2N)Fe_2(CO)_6$] (Fig. 12) [113].

The ADT bridge plays an important role in H_2 production in the natural system [116,117]. Diiron–ADT complexes have proved to be some of the best simple models for the active site of iron hydrogenases [106]. In the expected light-driven process, the photoexcited porphyrin is oxidatively quenched by the diiron unit to

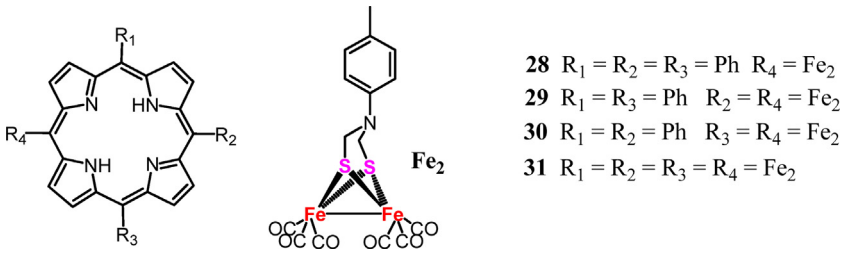

28 $R_1 = R_2 = R_3 = Ph$ $R_4 = Fe_2$
29 $R_1 = R_3 = Ph$ $R_2 = R_4 = Fe_2$
30 $R_1 = R_2 = Ph$ $R_3 = R_4 = Fe_2$
31 $R_1 = R_2 = R_3 = R_4 = Fe_2$

Fig. 12. Biomimetic models **28**–**31** for the active site of iron-hydeogenase.

give a reduced iron species. After regeneration of the porphyrin by electron transfer from an external donor, this process is repeated to produce a doubly reduced diiron species that should be able to drive the reduction of protons to hydrogen.

The same group synthesized a series of new light-driven models containing a porphyrin moiety covalently bound to a single diiron-ADT unit (**28**) or two (**29**, **30**) or four diiron-ADT units (**31**) (Fig. 12) [118]. It was found that H_2 was produced when irradiating ($\lambda > 400$ nm) a CH_2Cl_2 solution containing model **28**, ethanethiol (EtSH) as electron donor, and trifluoroacetic acid (TFA) as the proton source. A possible pathway for such photoinduced H_2 production is suggested, which involves an intramolecular electron transfer process from the photoexcited porphyrin moiety to the catalytic diiron-ADT unit.

Wasielewski and coworkers studied a naphthalene monoimide (NMI) dithiolate ligand for the diiron proton reduction catalyst in photodriven systems (**32**) and also the related dyad system featuring a covalently attached porphyrin chromophore (**33**) (Fig. 13) [119].

Photochemical hydrogen production experiments were performed by irradiating **33** (2 μmol) in the presence of TFA (2 mmol) in toluene and hydrogen gas (0.9 μmol) was generated. In the absence of either TFA or light, no H_2 production was detected. However, photochemical H_2 generation from TFA using **33** was not catalytic (turnover number of ~0.5). Addition of a *p*-anisidine sacrificial donor (2 mmol) significantly decreased the H_2 formation (0.02 μm). This fact was attributed to *p*-anisidine protonation, that greatly diminished both its electron donor ability and the TFA concentration. In a further study, Wasielewski and coworkers synthesized triads **34** and **35** bearing a ferrocene (Fc) as a secondary electron donor either directly linked or via a phenyl ring (Fig. 14) [120].

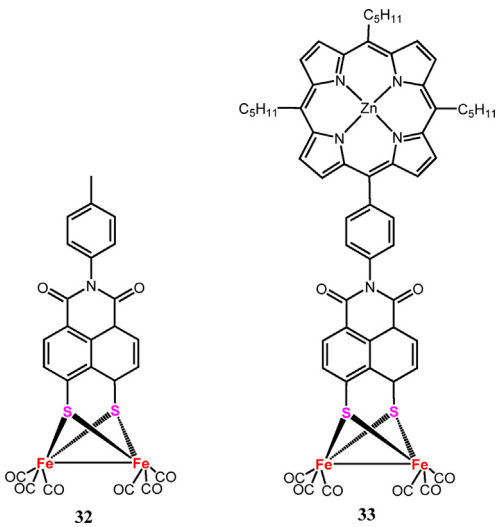

32 **33**

Fig. 13. Chemical structures of compounds **32** and **33**.

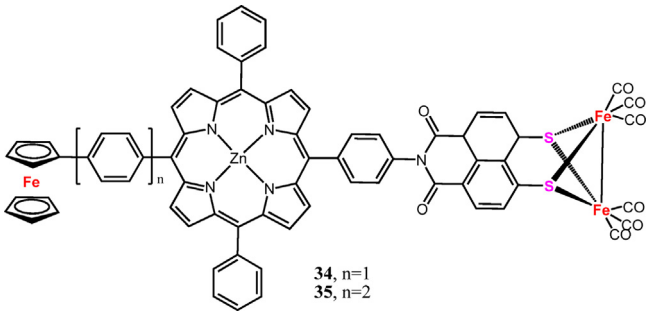

Fig. 14. Molecular structures of **34** and **35**.

A two-step, photoinitiated charge separation occurs in triads **34** and **35** in CH_2Cl_2; however, energy transfer from ^{1*}ZnTPP to Fc competes very efficiently with electron transfer from ^{1*}ZnTPP to [NMI-Fe^{I}-Fe^{I}-$S_2(CO)_6$], so that the yield of Fc^+–ZnTPP-[NMI-Fe^0-Fe^{I}-$S_2(CO)_6$] is only 13% and charge recombination occurs in 9 ns. In contrast, the simple insertion of an additional phenyl group between ZnTPP and Fc slows down the energy transfer rate from ^{1*}ZnTPP to Fc of about 20 times allowing the desired reduction of the diiron complex to dominate, so that the overall yield of Fc^+–Ph-ZnTPP-[NMI-Fe^0-Fe^{I}-$S_2(CO)_6$] rises to 71% and the charge recombination slows down to 67 ns. As a consequence, hydrogen production was observed only for triad **35** and not for triad **34**, though with TONs < 1.

Song and coworkers reported on compound **36**, in which the diiron ADT type complex [(μ-SCH_2)$_2$NC(O)C_5H_4N]-$Fe_2(CO)_6$ is bound to a ZnTPP photosensitizer via axial coordination of a peripheral pyridyl group to the Zn(II) center (Fig. 15) [121].

The fluorescence spectrum of **36**, in comparison with that of ZnTPP alone, indicated the occurring of an intramolecular electron transfer process from the photoexcited ZnTPP moiety to the coordinatively bound diiron complex. Studies of the catalytic ability by **36** towards the HER, however, were not present in this report.

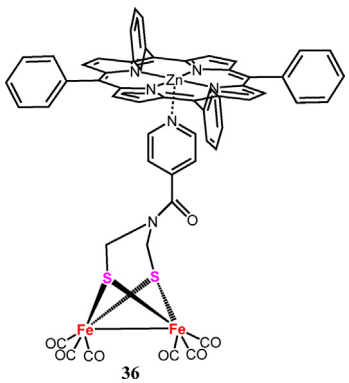

36

Fig. 15. Molecular structure of catalyst **36**.

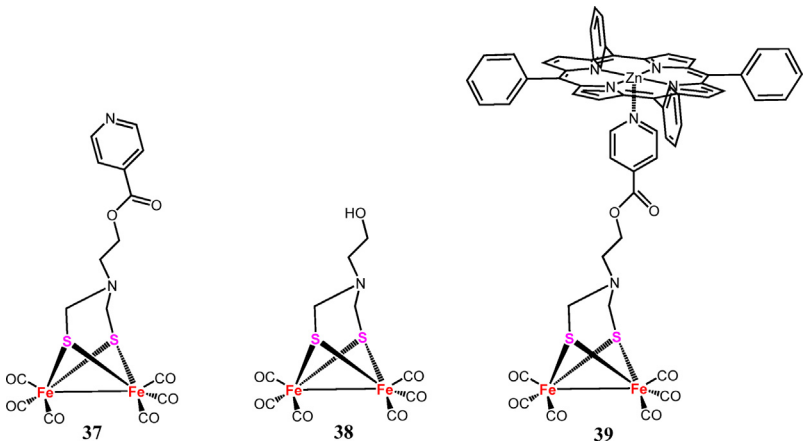

Fig. 16. Structures of the [2Fe2S] complexes **37** and **38** and supramolecular assembly **39**.

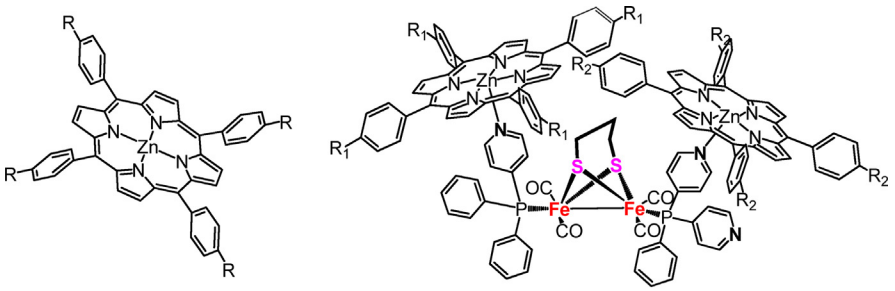

Fig. 17. Molecular structures of compounds **40**–**42**.

A similar non-covalent assembly, **39**, based on a ZnTPP and the iron hydrogenase active-site model **37** self-assembled via axial coordination, was reported by Sun and coworkers (Fig. 16) [122]. The studies on the assembly, also in comparison with the model systems **38** and ZnTPP, showed fast photo-induced intramolecular electron transfer from the excited singlet state of the zinc porphyrin to the diiron center. The assembled system proves to be superior to the intermolecular and to the covalently linked molecular dyads, since it can effectively reduce the detrimental charge recombination via complex dissociation. As a consequence, visible light-driven H_2 generation was observed from this self-assembled system with TON = 0.16 based based on **37** and TON = 16 based on ZnTPP. Also, there was no hydrogen evolved if **37** was replaced by **38**, in which the pyridyl group was replaced by an hydroxyl group unavailable for coordination to the chromophoric unit (Fig. 16). These results indicate that the assembly of **37** and ZnTPP via axial coordination is crucial for light-driven H_2 generation, and that intramolecular photoinduced ET does occur in **39**.

A supramolecular building block approach was introduced by Kluwer and coworkers where pyridyl-functionalized phosphine ligands coordinate with phosphorus to the active metal center, whereas the nitrogen donor coordinates selectively to chromophores such as zinc porphyrins (**40** and **41**) yielding the supramolecular assembly **42** (Fig. 17) [123].

Catalyst **42** photogenerated significant (TON = 5 with respect to the cluster concentration) amounts of H_2 gas in the presence of 2 molar equiv. of both **40** and **41**. Under these conditions, mixed assemblies with two different chromophores are likely formed. This observation suggests that the hydrogen-producing system requires the presence of both chromophores (**40** and **41**) in solution.

2.3. Porphyrin as sensitizers with cobalt complexes as catalysts

One of the first uses of porphyrin sensitizers coupled to cobalt complexes for hydrogen production from water was reported by Sun and coworkers [124]. These molecular devices consist of a porphyrin moiety as the sensitizer and a cobaloxime complex as the hydrogen evolving catalyst (Fig. 18) [33,41,125,126]. Three

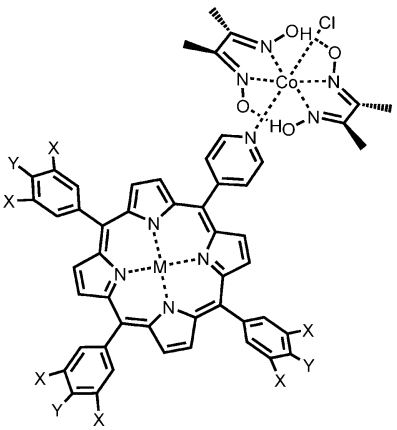

Fig. 18. Molecular structures of compounds **43**–**49**.

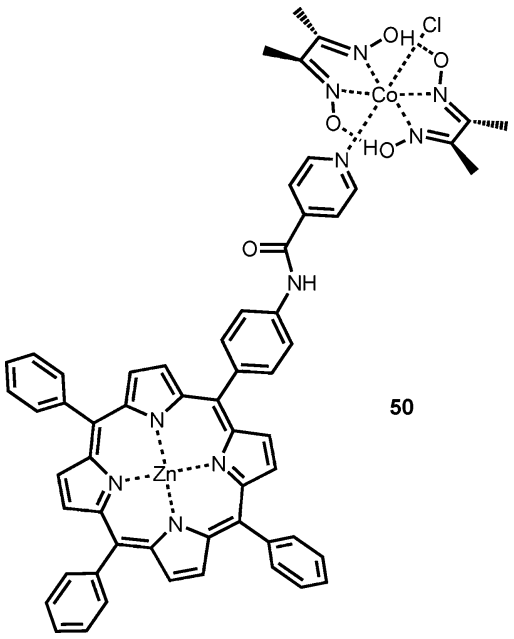

50

Fig. 19. Molecular structure of compound **50**.

different porphyrin derivatives with a pyridyl group at one *meso* position, namely a Zn(II), Mg(II), and a free-base porphyrin, were used to bind axially to the cobalt center of the catalytic moiety to construct three molecular dyads for photochemical hydrogen production (**43**, **44**, and **45**, respectively). Upon continuous visible irradiation in the presence of triethylamine (TEA) as sacrificial electron donor in a 80/20 THF/H_2O mixture, significant hydrogen evolution was observed only for the Zn(II)-substituted compound **43** (TON = 22 after 5 h), while only trace amounts were detected for the remaining complexes **44**, **45**. Hydrogen production was hypothesized to proceed through two subsequent intramolecular electron transfer processes from the singlet excited state of the porphyrin to the cobaloxime catalyst thus forming the active Co(I) species, with the recovery of the oxidized sensitizer at each electron transfer step promoted by the TEA donor. To this respect, the best hydrogen evolving performance by the zinc-substituted complex **43** was claimed to arise from (i) a larger driving force for the photoinduced electron transfer to the catalyst (favoring **43** and **44** with respect to **45**) and (ii) the possibility of an inner-sphere electron transfer process from the donor to the sensitizer due to pre-coordination of the TEA to the zinc metal center (favoring **43** with respect to both **44** and **45**). The same authors reported [127] other two molecular dyads (**46** and **50**) based on the very same cobalt catalyst and two different Zn(II) porphyrin sensitizers differing from **43** essentially for the lack of *tert*-butyl functional groups in the phenyl rings (**46**) and for the presence of a 4-isonicotinamidyl(phenyl) bridge instead of the pyridyl group (**50**) (Fig. 19). Complexes **46** and **50** showed improved photocatalytic activity (80/20 THF/H_2O, TEA as sacrificial donor) with respect to the parent compound **43** with overall TON after 12 h irradiation of 46 and 35, respectively. The lower activity observed for **50** with respect to **46** was mainly attributed to the longer sensitizer/catalyst distance slowing down the electron transfer process to the cobaloxime.

Almost simultaneously Guldi, Coutsolelos and coworkers [128] and Scandola and coworkers [129,130] beside testing the photocatalytic properties, addressed careful spectroscopic studies on very similar porphyrin-cobaloxime devices mainly differing from the ones studied by Sun and coworkers [124,127] for the presence of 4-carboxymethyl(phenyl) groups at the porphyrin *meso* position (**47**, **48**) [128] or for the presence of an aluminum(III) metal center in the porphyrin core **49** (Fig. 18) [129,130]. In both cases very fast, subnanosecond quenching processes of the porphyrin singlet excited state within the formed sensitizer/catalyst dyads were observed by time-resolved emission techniques [129,130]. More detailed investigation of the quenching process by means of time-resolved absorption spectroscopy allowed shedding more light into the quenching mechanism: Fast, monoexponential decay of the singlet excited state transient absorption features were observed for all the porphyrin–cobaloxime dyads [129,130]. This was ascribed to a fast oxidative photoinduced electron transfer from the singlet excited state of the porphyrins to the cobaloxime catalyst followed by a much faster charge recombination process which prevents eventual reaction with the sacrificial electron donor. Driving force and solvent effects on the charge separation rates were all compatible with this mechanism. More recently, by means of a different experimental/theoretical approach Pryce, Vos and coworkers suggested [131] that the fluorescence quenching by the cobaloxime catalyst is ascribable rather than to an electron transfer mechanism to an energy transfer to a lower energy cobaloxime-based excited state involving Co-N(pyridyl) bond lengthening and thus catalyst/sensitizer dissociation. Regardless of the mechanism, all these investigations converged to the idea that porphyrin quenching by cobaloxime is detrimental to photoinduced hydrogen evolution and cast several doubts on the previous reported hydrogen evolving activity by porphyrin–cobaloxime dyads or at least on the proposed photocatalytic mechanism [124,127]. As a matter of fact both Guldi and Coutsolelos [128] and Pryce and Vos [131] observed negligible amounts of hydrogen produced and thus failed to reproduce the data reported by Sun and coworkers [124,127].

A particular case of porphyrin–cobaloxime dyads is that reported by Scandola and coworkers [129] (dyad **49**) where the additional presence of a Lewis acid site in the porphyrin core, i.e. an aluminum center, triggered the formation of a photocatalytic reductant/sensitizer/catalyst triad taking advantage of ascorbic acid as sacrificial electron donor. Sizeable amounts of hydrogen were indeed produced upon continuous visible irradiation of the triad system (70/30 acetone/H_2O mixtures) with TON up to 352 and TOF up to 10.8 min^{-1} with respect to the sensitizer (quantum yield $\Phi = 0.046$) under optimized conditions [130]. The main conclusions from this study, however, were that association of the three components is not useful toward photoinduced hydrogen production, as in the mixed solvent used for the photocatalytic experiments the association of the three components is not complete and hydrogen formation arises from a bimolecular reaction of the triplet state of free aluminum(III) porphyrin sensitizer present in solution with the sacrificial donor. This primary photoreaction produces the reduced photosensitizer, which further reacts bimolecularly with the catalyst, thereby triggering hydrogen generation.

An homogeneous system involving a porphyrin sensitizer and a cobaloxime catalyst for photoinduced hydrogen evolution from water was recently reported by Weinstein, Coutsolelos and coworkers [132]. The system takes advantage of a water-soluble tetracationic zinc porphyrin (**9**) as sensitizer, an H-bridge cobalt(III) cobaloxime catalyst bearing a pyridine and a chloride as axial ligands (**51**) (Fig. 20), and TEOA as sacrificial electron donor. Upon continuous visible irradiation of mixed 50/50 acetonitrile/H_2O solutions hydrogen production was detected with the best result obtained at pH 7 with a TON of 280 with respect to the porphyrin after 35 h. Decomposition of both the sensitizer and the catalyst was responsible for the ceasing of the photocatalytic activity. Additional hints were also provided to shine light on the photoreaction mechanism: An oxidative quenching pathway was indeed deduced on the basis on transient absorption experiments. No singlet quenching by both the TEOA and the cobaloxime catalyst was observed. On the other hand, the tetracationic zinc porphyrin **9** reacts bimolecularly at the triplet level with the cobaloxime, the TEOA sacrificial

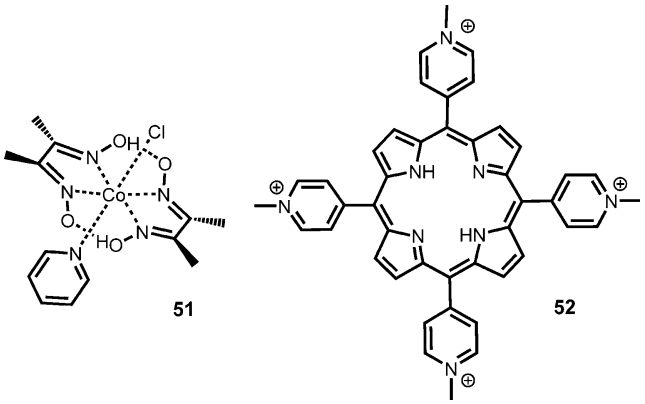

Fig. 20. Molecular structures of compounds **51** and **52**.

donor then recovers the oxidized sensitizer which is then capable of a second photoinduced reduction step on the catalyst with the formation of an active Co(I) species (also detected by conventional stationary absorption technique) capable of proton reduction to dihydrogen.

Photocatalytic activity was also observed for a similar system involving a tetracationic free-base porphyrin **52** (Fig. 20) as chromophore instead of the zinc analog, although the performance was remarkably lower (TON = 60 after 9 h irradiation) most likely as the result of the triplet excited state of the free-base porphyrin being a less powerful reducing agent than that of the zinc porphyrin [133].

3. Porphyrins as hydrogen evolving catalysts

As observed in the previous sections, the porphyrin macrocycle offers a unique platform for the coordination of different closed-shell metal centers, such as Zn(II), Al(III), Sn(IV), and Mg(II), with the possibility of tuning both the spectroscopic and electrochemical properties of the chromophore. On the other hand, the porphyrin macrocycle can be also employed for the stabilization of redox-active metal centers capable of evolving through different oxidation states with potential application in catalysis. In the quest of artificial photosynthesis several examples of such a use can be found in the literature regarding water splitting, for both water oxidation [134,135] and hydrogen production (see below), as well as CO_2 reduction [136–138].

As far as the hydrogen evolution reaction (HER) is concerned, one of the first studies which pointed out the actual potential of porphyrin macrocycles as catalysts was reported by Collman and coworkers [139] when investigating on the dihydrogen elimination reaction from osmium(II) and ruthenium(II) metalloporphyrin hydrides. Stable anionic hydrides, such as **53** and **54** (as monopotassium salts) (Fig. 21), were observed to undergo quantitative dihydrogen elimination either upon addition of equimolar amounts of benzoic acid or excess water in THF or upon chemically or electrochemically induced oxidation. While in the former case, experiments in deuterated water suggested dihydrogen formation

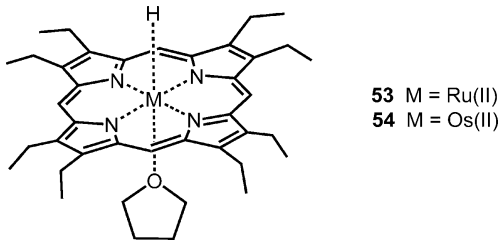

Fig. 21. Molecular structures of compounds **53** and **54**.

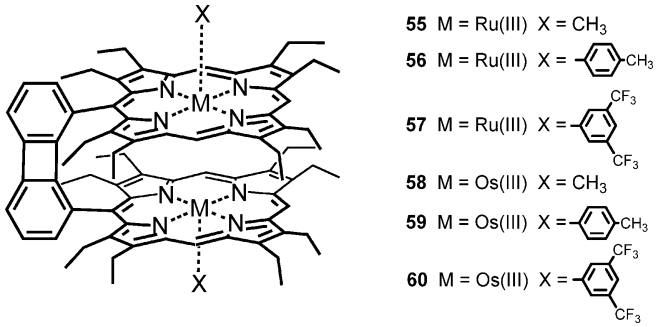

Fig. 22. Molecular structures of compounds **55**–**60**.

to occur through protonation of the hydride species, in the latter a bimolecular mechanism involving cooperation of two M(III)-H moieties was the dominating pathway [139].

The different metal center was observed to markedly affect the kinetic of dihydrogen elimination, but not the mechanism, with the ruthenium complex **53** being faster than the osmium analog **54**. Interestingly, the substitution of the axial THF with ligands with increasing trans-effect enhanced the rate of hydrogen elimination by both protonation of the M(II)-hydride and bimolecular elimination from the M(III)-hydride. Along this line, again Collman and coworkers [140] reported on the electrocatalytic hydrogen evolution from a series of cofacial bisorganometallic diporphyrin complexes **55**, **56**, and **57** and **58**, **59**, and **60**, differing essentially from the metal centers (ruthenium(III) or osmium(III), respectively) and the axial organic substituents (Fig. 22).

Electrochemical investigation at an Hg-pool electrode of THF solutions upon addition of acid showed that hydrogen is catalytically produced after two subsequent reduction steps involving both metal centers (i.e., formation of two M(II) species). Importantly, the change of the X substituent along the series **55**, **56**, **57** and **58**, **59**, **60** has a strong impact on the reduction potential of the metal centers and thus on the potential required to promote hydrogen formation, with compounds **57** and **60** reducing at less negative potentials than **56**, **59** and **55**, **58**. The basicity of the metal centers, however, is strictly related to the reduction potentials with the consequence that only catalysts having more negative reduction potentials (for instance **57** and **60**) can foster proton reduction in the presence of weak acids such as benzoic acid, whereas metalloporphyrin catalysts **55** and **56**, which have the least negative reduction potentials require stronger acid such as TFA to promote hydrogen evolution. As a matter of fact a straightforward correlation was observed between the strength of the acid required to protonate the electrochemically generated double-reduced species of the complexes and the electronic nature of the metal (with the related axial ligand) [140]. Bulk electrolysis experiments on THF solutions containing different proton sources give TONs between 1.6 and 5.5. The change of either the metal or the axial substituent has no remarkable impact on the overpotential for the HER, while it slightly affects the stability of the system under applied external potential with the osmium complexes resulting slightly more active than the ruthenium analogs. As regarding the hydrogen evolution mechanism, two possible pathways were proposed: (i) a mechanism involving formation of a dihydride intermediate then capable of eliminating hydrogen and (ii) a single-site process in which protonation and elimination take place at one single metal center assisted by electron transfer from the nearby metal anion species. Regardless of the actual pathway, an enhanced catalytic performance was observed with respect to the mononuclear species, suggesting that a contribution from the cofacial orientation is indeed important.

More appealing, noble-metal free porphyrin HER catalysts were also reported in the last decades. One example is the iron(III)

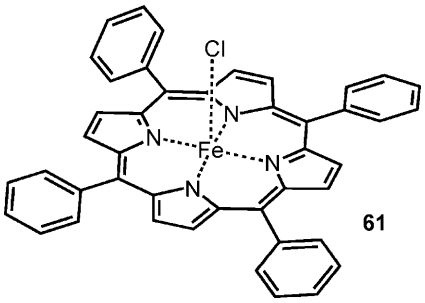

Fig. 23. Molecular structure of compound **61**.

tetraphenylporphyrin **61** (Fig. 23) studied by Savéant and coworkers [141]. Electrochemical investigation under cathodic scan in DMF solution shows the presence of three reversible one-electron reduction processes ascribable to the Fe(III)/Fe(II), Fe(II)/Fe(I), and Fe(I)/Fe(0) redox couples, respectively. Addition of protonated triethylamine triggers the appearance of a catalytic wave at potential values close to the Fe(I)/Fe(0) redox couple (onset at ca. −1.4 V vs. SCE), ascribable to proton reduction. Hydrogen production was observed upon bulk electrolysis at −1.6 V vs. SCE of a 50 mM Et_3NHCl (protonated triethylamine) DMF solution containing 1 mM **61** with a TON of 22 obtained after 1 h. Importantly, formation of hydrogen is selective with a Faradaic yield close to 100% and the linear relationship of charge vs. time suggests good stability of the catalyst within this timeframe. As far as the hydrogen evolution mechanism is concerned, proton attack on the Fe(II)–H catalytic intermediate, obtained through protonation of a Fe(0) species, is the rate-determining step of the overall catalysis which is mainly limited by diffusion of protons to the electrode surface. Despite the remarkable activity for the HER, the high negative operating potential of the catalyst strongly prevents its application within light-activated processes for photochemical water splitting.

To this respect cobalt porphyrins represent more suitable molecular components in view of practical uses. A first study dealing with cobalt porphyrins as hydrogen evolving molecular catalysts was reported in 1985 by Kellett and Spiro [142]. Three cobalt(II) porphyrins **62**, **63**, and **64** (Fig. 24) were shown to produce hydrogen from 0.1 M TFA aqueous solutions under application of −0.95 V vs. SCE at an Hg-pool electrode with a Faradaic yield close to 100%. Hydrogen evolving activity was observed to be mainly limited by adsorption of the porphyrin compounds at the electrode surface, a condition which also prevented any reliable kinetic and mechanistic investigations of the hydrogen evolving ability of cobalt porphyrins [142]. To this respect, however, the authors considered the formation of a Co(III)–H species through protonation of a Co(I) species as a key, initial step and provided two alternative mechanisms for the evolution of the latter toward hydrogen formation: (i) a heterolytic pathway involving protonation of the Co(III)–hydride intermediate and (ii) a homolytic pathway involving bimolecular reaction of two Co(III)–H species. On the basis of thermodynamic considerations and by comparison with analogous

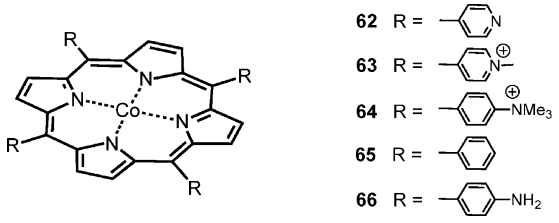

Fig. 24. Molecular structures of compounds **62**–**66**.

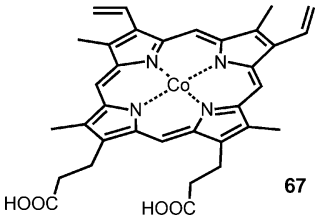

Fig. 25. Molecular structure of compound **67**.

cobalt-based catalytic systems [143], the authors concluded that the bimolecular mechanism (ii) is the dominant pathway.

In a follow-up study, the very same authors reported the tentative incorporation of cobalt porphyrin complexes on electrode surfaces by exploiting different strategies and techniques [144]. First, a cobalt tetraphenylporphyrin (**65**) was put on a glassy carbon (GC) electrode by drop-casting of a chloroform precursor solution. Second, the functionalized cobalt porphyrin **66** was covalently linked to a GC electrode through condensation reactions forming amide functional groups after conversion of surface carboxylic acid groups into acyl chloride ones. Third, porphyrin **62** was copolymerized in the presence of *p*-xylil α,α′-dibromide to form a cross-linked polycationic polymer. Fourth, a cobalt protoporphyrin IX **67** (Fig. 25) was electropolymerized via the peripheral vinyl substituents on the electrode surface. Fifth, both cationic compounds **63** and **64** were anchored on the GC electrode surface after incorporation within a negatively charged Nafion® membrane. The first four approaches failed to give stable, working electrodes mainly because of either desorption processes or stability issues under hydrogen evolving conditions. Only the **63**/**64** Nafion® films on GC were found to show substantial activity for the HER. In a 0.1 M TFA aqueous solution upon application of a cathodic potential of −0.95 V vs. SCE hydrogen was produced with a TON of 26 after 90 min of continuous electrolysis, however with remarkably low efficiency (ca. 30%) [144].

More recently, Nocera and coworkers reported on the electrochemical hydrogen evolution from organic acids catalyzed by a "hangman" cobalt(II) porphyrin **68** (Fig. 26) [145]. "Hangman" cobalt(II) porphyrin **68** and its molecular model **69** catalyze hydrogen production from a 15 mM benzoic acid solution in acetonitrile at an overpotential of ca. 800 mV and with Faradaic efficiencies between 80 and 85%. Despite the not outstanding catalytic properties, this work provided an essential mechanistic insight into the hydrogen evolving reaction catalyzed by cobalt porphyrins. Electrochemical investigation in acetonitrile solution in the presence of benzoic acid shows that cobalt(II) porphyrins **68** and **69** undergo a reversible one-electron Co(II)/Co(I) reduction at −1.10 V vs. Fc/Fc^+, which is followed by the catalytic proton discharge which falls at less negative potentials by ca. 120 mV in the case of **68** than for **69** (−1.90 V vs. Fc/Fc^+ and −2.02 V vs. Fc/Fc^+) as a result of the

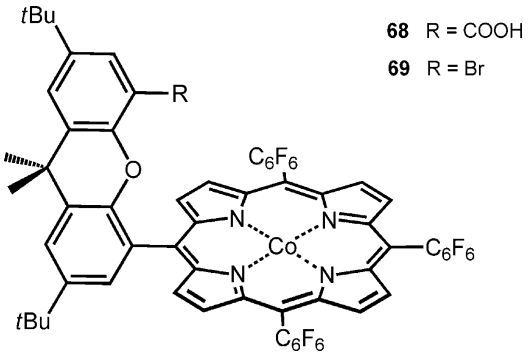

Fig. 26. Molecular structures of compounds **68** and **69**.

presence of the hanging group in **68** facilitating the formation of a Co(II)-hydride intermediate via intramolecular proton transfer. Therefore in these conditions hydrogen production does not take place upon protonation of the Co(I) species and an additional reduction/protonation step is required. This is likely the consequence of the presence of electron withdrawing groups at the *meso* positions decreasing the basicity of the electrochemically generated Co(I) species. Interestingly, in the presence of a stronger acid such as tosic acid the catalytic wave starts at the same, less negative potential (ca. −1.5 V vs. Fc/Fc^+) for both **68** and **69**, indicating that the "hangman" effect is bypassed. Under these strong acidic conditions, however, proton reduction catalysis still occurs at more negative potentials than the (now irreversible) Co(II)/Co(I) redox process, thus demontrating that the mechanism involves protonation of the Co(I) species yielding a Co(III)–hydride which, however, needs to be subsequently reduced to a Co(II)–H species capable of hydrogen evolution upon protonation [145].

The clear elucidation of the hydrogen evolution mechanism catalyzed by the "hangman" cobalt(II) porphyrin represented a powerful tool for better understanding the HER mechanism by the tetracationic cobalt(II) porphyrin **63** studied by Natali and coworkers [146] in both acetonitrile (with benzoic acid as proton donor) and neutral aqueous solutions (phosphate buffer, pH 7). In both cases catalytic water discharge is observed with an onset at ca. −1.2 V vs. SCE, at a more negative potentials than the Co(II)/Co(I) redox couple, thus implying that catalytic hydrogen evolution by **63** takes place only upon reduction and protonation of a Co(I) species. Interestingly, the relatively high potential of the proton reduction discharge paved the way for the investigation of such a tetracationic cobalt(II) porphyrin **63** as a molecular catalyst powered within a light-activated photocatalytic cycle. As a matter of fact Natali and coworkers reported [146] that **63** is a competent molecular catalyst for hydrogen generation from phosphate buffer solutions (pH 7) upon continuous visible irradiation in the presence of $Ru(bpy)_3^{2+}$ as photosensitizer and ascorbic acid as sacrificial electron donor achieving TON up to 725 mainly limited by depletion of the catalyst **63** [146]. As shown by time-resolved spectroscopy, reduction of the cobalt porphyrin catalyst takes place after reductive quenching of the $Ru(bpy)_3^{2+}$ chromophore by ascorbic acid and subsequent electron transfer to **63**. The first electron transfer event takes place at a remarkable rate, close to the diffusion limit, an important condition to prevent undesired parasite reactions involving the reduced species of the sensitizer produced under continuous irradiation.

In the context of hydrogen evolution catalysis by means of macrocyclic cobalt complexes, particular attention has been also devoted to other macrocycles such as corroles. Corroles are synthetic tetrapyrrolic macrocycles from the porphyrinoid family, but have several important differences with respect to porphyrins: (i) the macrocycle is a trianionic ligand and as such has the tendency to coordinate trivalent metal centers, (ii) the ring cavity is smaller than that of a porphyrin and thus can accommodate smaller metal centers which usually sit out of the plane of the aromatic structure, (iii) corroles are electron-rich molecules and are usually stabilized by insertion of electron-withdrawing groups at the ring periphery [147].

In a close similarity with cobalt porphyrins, cobalt(III) corroles have been used as electrocatalysts for water oxidation [148,149] as well as for the hydrogen evolving reaction [149–151]. As far as the latter is concerned, Gross and Dey reported electrocatalytic hydrogen production with several cobalt corroles (**70**, **71**, **72**) (Fig. 27), featuring different susbtituents at the β-pyrrole positions [150,151]. Electrochemical investigation in acetonitrile solution in the presence of TFA as proton source showed that the cobalt corrole undergoes a first Co(III)/Co(II) reduction, whose irreversible behavior was attributed to detachment of the axial pyridine, which is then followed by the catalytic discharge near the potentials of

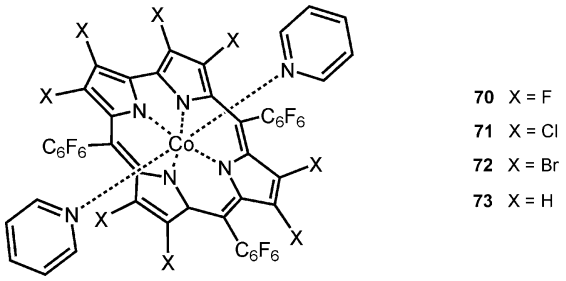

Fig. 27. Molecular structures of compounds **70**–**73**.

the Co(II)/Co(I) couple. The presence of different functional groups at the β-pyrrole positions has a remarkable impact on the electrocatalytic properties of the cobalt(III) corrole catalyst. First, the onset of the catalytic wave shifts to more negative potentials in the order **72** > **71** > **70** (−0.40, −0.55, −0.60 V vs. Ag/AgCl, respectively), directly correlating with the reduction potential of the Co(II)/Co(I) redox couple along the series. Second, estimation of the kinetic reactivity toward proton reduction explored at different TFA concentrations shows that the most active catalyst is the fluorinated substituted **70**, followed by the chlorinated analog **71** and the brominated **72**. As far as the catalytic mechanism is concerned, a combined ^{19}F NMR and theoretical investigation reveals that formation of a Co(III)–H species, obtained through two consecutive reduction of the cobalt center from Co(III)-to-Co(II)-to-Co(I) and subsequent protonation, is the rate-determining step. The Co(III)–H intermediate may then release hydrogen either by protonation (heterolythic pathway) or via disproportionation (homolythic pathway).

The β-pyrrole unsubstituted cobalt(III) corrole **73** was also used by Du, Lai, and Cao [149] for coating a GC electrode to achieve electrocatalytic proton reduction. Electrochemical investigation of the so-formed electrode showed the onset of a catalytic wave at −0.85 V vs. Ag/AgCl, about 250 mV more negative with respect to the fluorinated analog **70** due to the shift of the Co(II)/Co(I) redox process toward higher cathodic potentials [150,151]. The electrode was active toward hydrogen evolution with Faradaic efficiencies up to 96%, obtained upon bulk electrolysis experiment in a 0.5 M H_2SO_4 solution at a holding potential of −1.00 V vs. Ag/AgCl. Moreover, recovery of the catalyst **73** after 9-h electrolysis showed negligible decomposition during catalysis [149], an important feature for potential application in large scale devices.

In summary porphyrinoid complexes of redox active metal centers such as Co, Fe, Ru, and Os pose as competent molecular catalysts for the HER from organic solvents in the present of suitable proton sources as well as from purely aqueous solutions, even if the required overpotential to drive the HER usually lies at higher values in comparison with other active metal complexes [152]. This notwithstanding, the general synthetic ease of such compounds, with the possibility of changing the nature of the inner metal centers, as well as the substituents in both the *meso*- and β-positions, allows for a wide tunability of the redox properties with important implications toward the optimization of the catalytic performance. Moreover, the presence of a delocalized π-system involving the macrocycle may help to stabilize low-valence redox states of the metal (which are implicated in the HER catalysis) thanks to the partial delocalization of the negative charge on the aromatic ring [145]. Although this might be of particular importance toward an efficient hydrogen production, however, the partial involvement of the aromatic ring in the redox reactions is likely to affect the stability of the catalyst under turnover conditions [146]. Disproportionation reactions involving the reduced systems are indeed probable, undesired, parasite pathways occurring during catalysis with important effects on the overall catalytic performance.

Finally, the chromophoric nature of porphyrinoid compounds represents a possible drawback in view of the employment of such systems as catalysts in photocatalytic experiments. Porphyrins display indeed strong absorptions in the visible, which can overlap with those of the sensitizer thus competing in light absorption with the latter. However, the possibility of working at highly diluted catalyst concentrations (usually in the micromolar range) may help to prevent such an undesired effect [146].

4. Conclusions

The work summarized in this review is quite varied, including systems with very different levels of complexity, performance, and mechanistic insight. In general, porphyrins and metalloporphyrin appear to perform as good photosensitizers for photocatalytic hydrogen production, comparable to more popular classes of sensitizers such as, e.g., ruthenium polypyridine dyes.

All the systems reviewed here, however different in complexity, belong to two distinct classes of mechanistic behavior: oxidative or reductive quenching, depending on whether the primary excited-state electron transfer process is from the sensitizer toward the HEC (with or without the intermediacy of relay molecules) or from the SED to the photosensitizer. Often, the actual emphasis on hydrogen production leaves relatively little room for experimental detailed inspection (photophysical measurements, detection of intermediates by time-resolved techniques) that could lead to clear mechanistic conclusions. For instance, in most of the systems using platinum metal as catalyst an oxidative quenching mechanism is more or less tacitly assumed. However, in the few systems where specific electrochemical or photophysical measurements were performed [48,60,68,81], a reductive quenching mechanism was found to be operative. Similar arguments apply to the systems using hydrogenase mimics as catalysts. In the systems using cobalt complexes as HECs, on the other hand, the reductive quenching pathway is largely prevailing, as shown by detailed mechanistic studies.

Porphyrins and metalloporphyrin sensitizers may in principle undergo photoinduced electron transfer either at the singlet or at the triplet level. This electron transfer is from the porphyrin to the catalyst – or to an appropriate relay – in an oxidative quenching mechanism and from the SED in a reductive quenching mechanism. Obviously, all singlet electron transfer processes are thermodynamically favored over the corresponding triplet ones (in porphyrin-based systems typically by ca 0.4–0.5 eV). The problem with singlet reactivity is, of course, related to the singlet lifetime which is usually too short (typically few ns) to allow efficient bimolecular processes to occur. In principle, this problem could be circumvented by having the sensitizer and the electron donor or acceptor linked in some kind of supramolecular structure, in order to make the processes unimolecular. In practice, with very few exceptions, the strategy has not proven to be very successful, as the photosensitizer is often oxidatively quenched by the catalyst in a fast process. Also, an even faster charge recombination takes place, preventing any further useful reactivity. As a result, very modest TONs of H_2 production are obtained. In fact, most of the successful, high TON hydrogen evolution experiments are bimolecular in nature, involving the long-lived triplet state of the porphyrin.

While playing mainly the role of photosensitizers, some porphyrin-based systems have also found application as HECs. These are systems containing transition metal centers such as Co, Fe, Ru, Os, in which the catalytic activity is related to their variety of easily accessible oxidation states. From this viewpoint, metal porphyrin and related species, with the additional stability provided by the macrocyclic ligand, are similar to other complexes of the same metals, in terms of both catalytic mechanism and performance. A possible drawback, specific to these porphyrin-based systems is their strong chromophoric character, which may cause competition for light absorption with the photosensitizer. At the relative concentrations used in photocatalytic experiments, however, this effect is usually negligible.

A practically relevant aspect, which is not often dealt with sufficient detail in this type of work, is the analysis of the factors that determine, after a given irradiation time, the photochemical hydrogen generating activity to cease. In principle, both photosensitizer and catalyst degradation may be involved, but very rarely specific experiments are reported to the purpose of disentangling the effects. In particular, as far as decomposition of the photosensitizer P is concerned, this may have to deal with the stability of the oxidized P^+ or reduced P^- form of the sensitizer, depending on the oxidative or reductive mechanism of the process. In both cases, the actual behavior will be mostly dependent on the rate at which the positive or negative charge is removed from P^+ by the SEA or from P^- by the catalyst (or by an appropriate relay). The faster these rates, the more stable and durable is expected to be the photocatalytic hydrogen evolving system. Therefore, the detailed kinetic characterization by means of time-resolved techniques is to be regarded not only as a powerful mechanistic tool, but also as a worthwhile means to obtain essential information for the optimization of practical performance.

Acknowledgements

This research is funded by the European Commission FP7-REGPOT-2008-1, Project BIOSOLENUTI No. 229927, Heraklitos grant from Ministry of Education, and GSRT. The Special Research Account of the University of Crete is also acknowledged. Financial support from the Italian MIUR (FIRB RBAP11C58Y "NanoSolar", PRIN 2010 "Hi-Phuture") and COST action CM1202 "PERSPECT-H2O" is gratefully acknowledged.

References

[1] A.L. Hammond, Science 177 (1972) 1088–1090.
[2] J.K. Dawson, Nature 249 (1974) 724–726.
[3] V. Balzani, L. Moggi, M.F. Manfrin, F. Bolletta, M. Gleria, Science 189 (1975) 852–856.
[4] N. Armaroli, V. Balzani, Chemsuschem 4 (2011) 21–36.
[5] J. Rifkin, The Hydrogen Economy: The Creation of the Worldwide Energy Web and the Redistribution of Power on Earth, Penguin Putnam, New York, 2003.
[6] D.A.J. Rand, R.M. Dell, Hydrogen Energy: Challenges and Prospects, RSC, Cambridge, 2008.
[7] A. Züttel, A. Borgschulte, L. Schlapbach (Eds.), Hydrogen as a Future Energy Carrier, Wiley-VCH, Weinheim, 2008.
[8] In practical systems, additional components can be present, in particular electron relays connecting the catalysts with the photosensitizer (vide infra).
[9] In practice a considerable fraction of the available energy must be burn out for kinetic reasons (to drive the process in the right direction, with the useful electron transfer steps fast enough to overcome excited-state deactivation and charge recombination). In natural photosynthesis this problem is solved by using the energy of two photons processes by of two photosystems connected in series.
[10] A. Sartorel, M. Bonchio, S. Campagna, F. Scandola, Chem. Soc. Rev. 42 (2013) 2262–2280.
[11] P.D. Tran, V. Artero, M. Fontecave, Energy Environ. Sci. 3 (2010) 727–747.
[12] M. Wang, L. Chen, L. Sun, Energy Environ. Sci. 5 (2012) 6763–6778.
[13] P.D. Tran, L.H. Wong, J. Barber, J.S.C. Loo, Energy Environ. Sci. 5 (2012) 5902–5918.
[14] P. Du, R. Eisenberg, Energy Environ. Sci. 5 (2012) 6012–6021.
[15] Y. Zhao, J.R. Swierk, J.D. Megiatto Jr., B. Sherman, W.J. Youngblood, D. Qin, D.M. Lentz, A.L. Moore, T.A. Moore, D. Gust, T.E. Mallouk, Proc. Natl. Acad. Sci. U. S. A. 109 (2012) 15612–15616.
[16] L. Alibabaei, H. Luo, R.L. House, P.G. Hoertz, R. Lopez, T.J. Meyer, J. Mater. Chem. A 1 (2013) 4133–4145.
[17] Y. Gao, X. Ding, J. Liu, L. Wang, Z. Lu, L. Li, L. Sun, J. Am. Chem. Soc. 135 (2013) 4219–4222.
[18] J.R. McKone, S.C. Marinescu, B.S. Brunschwig, J.R. Winkler, H.B. Gray, Chem. Sci. 5 (2014) 865–878.
[19] A.J. Bard, M.A. Fox, Acc. Chem. Res. 28 (1995) 141–145.

[20] P. Keller, A. Moradpour, E. Amouyal, H.B. Kagan, Nouv. J. Chim. 4 (1980) 377–384.
[21] J. Kiwi, M. Gratzel, Nature 281 (1979) 657–658.
[22] J.-M. Lehn, J.-P. Sauvage, Nouv. J. Chim. 1 (1977) 449–451.
[23] R. Abe, K. Sayama, H. Arakawa, J. Photochem. Photobiol. A 166 (2004) 115–122.
[24] R.P. Sabatini, T.M. McCormick, T. Lazarides, K.C. Wilson, R. Eisenberg, D.W. McCamant, J. Phys. Chem. Lett. 2 (2011) 223–227.
[25] D.G. Nocera, Acc. Chem. Res. 45 (2012) 767–776.
[26] D. Merki, H. Vrubel, L. Rovelli, S. Fierro, X. Hu, Chem. Sci. 3 (2012) 2515–2525.
[27] P.D. Tran, M. Nguyen, S.S. Pramana, A. Bhattacharjee, S.Y. Chiam, J. Fize, M.J. Field, V. Artero, L.H. Wong, J. Loo, J. Barber, Energy Environ. Sci. 5 (2012) 8912–8916.
[28] F. Gloaguen, T.B. Rauchfuss, Chem. Soc. Rev. 38 (2009) 100–108.
[29] D. Streich, Y. Astuti, M. Orlandi, L. Schwartz, R. Lomoth, L. Hammarström, S. Ott, Chem. Eur. J. 16 (2010) 60–63.
[30] T. Yu, Y. Zeng, J. Chen, Y.-Y. Li, G. Yang, Y. Li, Angew. Chem. Int. 52 (2013) 5631–5635.
[31] M. Rakowski DuBois, D.L. DuBois, Chem. Soc. Rev. 38 (2009) 62–72.
[32] M. Razavet, V. Artero, M. Fontecave, Inorg. Chem. 44 (2005) 4786–4795.
[33] J.L. Dempsey, B.S. Brunschwig, J.R. Winkler, H.B. Gray, Acc. Chem. Res. 42 (2009) 1995–2004.
[34] P. Du, J. Schneider, G. Luo, W.W. Brennessel, R. Eisenberg, Inorg. Chem. 48 (2009) 4952–4962.
[35] C.C.L. McCrory, C. Uyeda, J.C. Peters, J. Am. Chem. Soc. 134 (2012) 3164–3170.
[36] A. Juris, V. Balzani, F. Barigelletti, S. Campagna, P. Belser, A. von Zelewsky, Coord. Chem. Rev. 84 (1988) 85–277.
[37] B. Probst, M. Guttentag, A. Rodenberg, P. Hamm, R. Alberto, Inorg. Chem. 50 (2011) 3404–3412.
[38] E.D. Cline, S.E. Adamson, S. Bernhard, Inorg. Chem. 47 (2008) 10378–10388.
[39] P. Du, K. Knowles, R. Eisenberg, J. Am. Chem. Soc. 130 (2008) 12576–12577.
[40] First- and second-row transition metal complexes, because of the presence of low-lying d–d states, are usually too short lived to undergo efficient photoinduced electron transfer processes.
[41] T. Lazarides, T. McCormick, P. Du, G. Luo, B. Lindley, R. Eisenberg, J. Am. Chem. Soc. 131 (2009) 9192–9194.
[42] T.M. McCormick, Z. Han, D.J. Weinberg, W.W. Brennessel, P.L. Holland, R. Eisenberg, Inorg. Chem. 50 (2011) 10660–10666.
[43] D. Gust, T.A. Moore, A.L. Moore, in: V. Balzani (Ed.), Electron Transfer in Chemistry, vol. III, Part 2, Wiley-VCH, Weinheim, Germany, 2001, pp. 273–336 (Chapter 2).
[44] S. Fukuzumi, H. Imahori, in: V. Balzani (Ed.), Electron Transfer in Chemistry, vol II, Part 2, Wiley-VCH, Weinheim, Germany, 2001, pp. 927–966 (Chapter 8).
[45] M.R. Wasielewski, J. Org. Chem. 71 (2006) 5051–5066.
[46] K. Kalyanasundaram, J. Chem. Soc., Faraday Trans. 2 (79) (1983) 1365–1374.
[47] A. Harriman, G. Porter, P. Walters, J. Chem. Soc., Faraday Trans. 1 (79) (1983) 1335–1350.
[48] A. Harriman, J. Photochem. 29 (1985) 139–150.
[49] A. Harriman, G. Porter, J. Chem. Soc., Faraday Trans. 2 (75) (1979) 1532–1542.
[50] M. Gouterman, in: D. Dolphin (Ed.), The Porphyrins, vol. 3, Academic Press, New York, 1978 (Chapter 1).
[51] A. Harriman, G. Porter, M.-C. Richoux, J. Chem. Soc. Faraday Trans. 2: Mol. Chem. Phys. 77 (1981) 833–844.
[52] O. Mizuno, R. Dinsdale, F.R. Hawkes, D.L. Hawkes, T. Noike, Bioresour. Technol. 73 (2000) 59–65.
[53] V.R. Rustamov, K.M. Abdullayev, F.G. Aliyev, V.K. Kerimov, Int. J. Hydrogen Energy 23 (1998) 649–652.
[54] J. Woodward, M. Orr, K. Cordray, E. Greenbaum, Nature 405 (2000) 1014–1015.
[55] T. Inoue, S.N. Kumar, T. Kamachi, I. Okura, Chem. Lett. 28 (1999) 147–148.
[56] J. Woodward, S.M. Mattingly, M. Danson, D. Hough, N. Ward, M. Adams, Nat. Biotechnol. 14 (1996) 872–874.
[57] Y. Saiki, Y. Amao, Biotechnol. Bioeng. 82 (2003) 710–714.
[58] H. Yamaguchi, T. Onji, H. Ohara, N. Ikeda, A. Harada, Bull. Chem. Soc. Jpn. 82 (2009) 1341–1346.
[59] L. Zhang, Y. Lu, Y. Du, P. Yang, X. Wang, J. Porphyrins Phthalocyanines 14 (2010) 540–546.
[60] A. Fateeva, P.A. Chater, C.P. Ireland, A.A. Tahir, Y.Z. Khimyak, P.V. Wiper, J.R. Darwent, M.J. Rosseinsky, Angew. Chem. Int. Ed. 51 (2012) 7440–7444.
[61] M. Zhu, Y. Dong, Y. Du, Z. Mou, J. Liu, P. Yang, X. Wang, Chem. Eur. J. 18 (2012) 4367–4374.
[62] Z.-M. Lin, W.-Z. Feng, H.-K. Leung, J. Chem. Soc. Chem. Commun. (1991) 209–211.
[63] M. Zhu, Y. Lu, Y. Du, J. Li, X. Wang, P. Yang, Int. J. Hydrogen Energy 36 (2011) 4298–4304.
[64] H. Kotani, T. Ono, K. Ohkubo, S. Fukuzumi, Phys. Chem. Chem. Phys. 9 (2007) 1487–1492.
[65] M. Zhu, Y. Du, P. Yang, X. Wang, Catal. Sci. Technol. 3 (2013) 2295–2302.
[66] K. Kalyanasundaram, M. Grätzel, Helv. Chim. Acta 63 (1980) 478–485.
[67] E.A. Malinka, G.L. Kamalov, S.V. Vodzinskii, V.I. Melnik, Z.I. Zhilina, J. Photochem. Photobiol. A: Chem. 90 (1995) 153–158.
[68] W. Kim, T. Tachikawa, T. Majima, C. Li, H.-J. Kim, W. Choi, Energy Environ. Sci. 3 (2010) 1789–1795.
[69] S. Noda, H. Hosono, I. Okura, Y. Yamamoto, Y. Inoue, J. Chem. Soc., Faraday Trans. 86 (1990) 811–814.
[70] I. Okura, H. Hosono, Inorg. Chim. Acta 189 (1991) 145–147.
[71] I. Okura, H. Hosono, J. Phys. Chem. 96 (1992) 4466–4469.
[72] J. Hirota, I. Okura, J. Phys. Chem. Lett. 97 (1993) 6867–6870.
[73] M. Fujihira, K. Nishiyama, H. Yamada, Thin Solid Films 132 (1985) 77–82.
[74] Y. Cao, B.W. Zhang, W.Y. Qian, X.D. Wang, J.W. Bai, X.R. Xiao, J.G. Jia, J.W. Xu, Sol. Energy Mater. Sol. Cells 38 (1995) 139–155.
[75] H. Hosono, M. Kaneko, J. Photochem. Photobiol. A 107 (1997) 63–70.
[76] A. Harriman, G. Porter, M.-C. Richoux, J. Chem. Soc. Faraday Trans. 2 (77) (1981) 1939–1948.
[77] A. Harriman, M.-C. Richoux, J. Photochem. 15 (1981) 335–339.
[78] I. Okura, N.K. Thuan, J. Chem. Soc. Faraday Trans. 1: Phys. Chem. Condens. Phases 76 (1980) 2209–2211.
[79] H. Hosono, T. Tani, I. Uemura, Chem. Commun. (1996) 1893–1894.
[80] H. Hosono, J. Photochem. Photobiol. A: Chem. 126 (1999) 91–97.
[81] T. Abe, H. Imaya, M. Endo, M. Kaneko, Polym. Adv. Technol. 11 (2000) 167–171.
[82] P. Ngweniform, Y. Kusumoto, M. Ikeda, S. Somekawa, B. Ahmmad, Chem. Phys. Lett. 428 (2006) 436–439.
[83] M. Zhu, Z. Li, B. Xiao, Y. Lu, Y. Du, P. Yang, X. Wang, ACS Appl. Mater. Interfaces 5 (2013) 1732–1740.
[84] J.C. Fontecilla-Camps, A. Volbeda, C. Cavazza, Y. Nicolet, Chem. Rev. 107 (2007) 4273–4303.
[85] P.M. Vignais, B. Billoud, Chem. Rev. 107 (2007) 4206–4272.
[86] M. Frey, Chembiochem 3 (2002) 153–160.
[87] I. Okura, Coord. Chem. Rev. 68 (1985) 53–99.
[88] J.R. Darwent, P. Douglas, A. Harriman, G. Porter, M.-C. Richoux, Coord. Chem. Rev. 44 (1982) 83–126.
[89] I. Okura, N. Kim-Thuan, J. Mol. Catal. 6 (1979) 227–230.
[90] I. Okura, M. Takeuchi, N. Kim-Thuan, Photochem. Photobiol. 33 (1981) 413–416.
[91] I. Okura, M. Takeuchi, S. Kusunoki, S. Aono, Chem. Lett. 11 (1982) 187–188.
[92] N. Kaji, S. Aono, I. Okura, J. Mol. Catal. 36 (1986) 201–203.
[93] Y. Amao, I. Okura, J. Mol. Catal. B: Enzym. 17 (2002) 9–21.
[94] P.A. Brugger, P.P. Infelta, A.M. Braun, M. Gratzel, J. Am. Chem. Soc. 103 (1981) 320–326.
[95] I. Okura, T. Kita, S. Aono, N. Kaji, J. Mol. Catal. 32 (1985) 361–363.
[96] Y. Amao, Y. Tomonou, Y. Ishikawa, I. Okura, Int. J. Hydrogen Energy 27 (2002) 621–625.
[97] Y. Amao, I. Okura, J. Mol. Catal. A: Chem. 103 (1995) L69–L71.
[98] Y. Amao, I. Okura, J. Mol. Catal. A: Chem. 105 (1996) 125–130.
[99] Y. Amao, Y. Tomonou, I. Okura, Sol. Energy Mater. Sol. Cells 79 (2003) 103–111.
[100] D. Holten, D.F. Bocian, J.S. Lindsey, Acc. Chem. Res. 35 (2001) 57–69.
[101] H.G. Liu, D.J. Qian, X.S. Feng, Q.B. Xue, K.Z. Yang, Langmuir 16 (2000) 5079–5085.
[102] F. Armand, P.-A. Albouy, F. Da Cruz, M. Normand, V. Huc, E. Goron, Langmuir 17 (2001) 3431–3437.
[103] I. Prieto, J.M. Pedrosa, M.T. Martín-Romero, D. Möbius, L. Camacho, J. Phys. Chem. B 104 (2000) 9966–9972.
[104] D.-J. Qian, S.-O. Wenk, C. Nakamura, T. Wakayama, N. Zorin, J. Miyake, Int. J. Hydrogen Energy 27 (2002) 1481–1487.
[105] I. Okura, A. Miyaji, T. Kamachi, N. Asakura, J. Porphyrins Phthalocyanines 06 (2002) 26–32.
[106] S. Ott, M. Kritikos, B. Åkermark, L. Sun, R. Lomoth, Angew. Chem. Int. 43 (2004) 1006–1009.
[107] J.-F. Capon, F. Gloaguen, P. Schollhammer, J. Talarmin, Coord. Chem. Rev. 249 (2005) 1664–1676.
[108] S.J. Borg, T. Behrsing, S.P. Best, M. Razavet, X. Liu, C.J. Pickett, J. Am. Chem. Soc. 126 (2004) 16988–16999.
[109] R. Mejia-Rodriguez, D. Chong, J.H. Reibenspies, M.P. Soriaga, M.Y. Darensbourg, J. Am. Chem. Soc. 126 (2004) 12004–12014.
[110] Y. Na, J. Pan, M. Wang, L. Sun, Inorg. Chem. 46 (2007) 3813–3815.
[111] Y. Na, M. Wang, J. Pan, P. Zhang, B. Åkermark, L. Sun, Inorg. Chem. 47 (2008) 2805–2810.
[112] L. Sun, B. Åkermark, S. Ott, Coord. Chem. Rev. 249 (2005) 1653–1663.
[113] L.-C. Song, M.-Y. Tang, F.-H. Su, Q.-M. Hu, Angew. Chem. Int. Ed. 45 (2006) 1130–1133.
[114] M.R. Wasielewski, Chem. Rev. 92 (1992) 435–461.
[115] A.N. Macpherson, P.A. Liddell, D. Kuciauskas, D. Tatman, T. Gillbro, D. Gust, T.A. Moore, A.L. Moore, J. Phys. Chem. B 106 (2002) 9424–9433.
[116] Y. Nicolet, A.L. de Lacey, X. Vernède, V.M. Fernandez, E.C. Hatchikian, J.C. Fontecilla-Camps, J. Am. Chem. Soc. 123 (2001) 1596–1601.
[117] H.-J. Fan, M.B. Hall, J. Am. Chem. Soc. 123 (2001) 3828–3829.
[118] L.-C. Song, L.-X. Wang, M.-Y. Tang, C.-G. Li, H.-B. Song, Q.-M. Hu, Organometallics 28 (2009) 3834–3841.
[119] A.P.S. Samuel, D.T. Co, C.L. Stern, M.R. Wasielewski, J. Am. Chem. Soc. 132 (2010) 8813–8815.
[120] P. Poddutoori, D.T. Co, A.P.S. Samuel, C.H. Kim, M.T. Vagnini, M.R. Wasielewski, Energy Environ. Sci. 4 (2011) 2441–2450.
[121] L.-C. Song, M.-Y. Tang, S.-Z. Mei, J.-H. Huang, Q.-M. Hu, Organometallics 26 (2007) 1575–1577.
[122] X. Li, M. Wang, S. Zhang, J. Pan, Y. Na, J. Liu, B.r. Åkermark, L. Sun, J. Phys. Chem. B 112 (2008) 8198–8202.
[123] A.M. Kluwer, R. Kapre, F. Hartl, M. Lutz, A.L. Spek, A.M. Brouwer, P.W.N.M. van Leeuwen, J.N.H. Reek, Proc. Natl. Acad. Sci. U.S.A. 106 (2009) 10460–10465.
[124] P. Zhang, M. Wang, C. Li, X. Li, J. Dong, L. Sun, Chem. Commun. 46 (2010) 8806–8808.

[125] A. Fihri, V. Artero, M. Razavet, C. Baffert, W. Leibl, M. Fontecave, Angew. Chem. Int. 47 (2008) 564–567.
[126] F. Lakadamyali, E. Reisner, Chem. Commun. 47 (2011) 1695–1697.
[127] P. Zhang, M. Wang, X. Li, H. Cui, J. Dong, L. Sun, Sci. China Chem. 55 (2012) 1274–1282.
[128] K. Peuntinger, T. Lazarides, D. Dafnomili, G. Charalambidis, G. Landrou, A. Kahnt, R.P. Sabatini, D.W. McCamant, D.T. Gryko, A.G. Coutsolelos, D.M. Guldi, J. Phys. Chem. C 117 (2012) 1647–1655.
[129] M. Natali, M. Orlandi, C. Chiorboli, E. Iengo, V. Bertolasi, F. Scandola, Photochem. Photobiol. Sci. 12 (2013) 1749–1753.
[130] M. Natali, R. Argazzi, C. Chiorboli, E. Iengo, F. Scandola, Chem. Eur. J. 19 (2013) 9261–9271.
[131] J.C. Manton, C. Long, J.G. Vos, M.T. Pryce, Dalton Trans. 43 (2014) 3576–3583.
[132] T. Lazarides, M. Delor, I.V. Sazanovich, T.M. McCormick, I. Georgakaki, G. Charalambidis, J.A. Weinstein, A.G. Coutsolelos, Chem. Commun. 50 (2013) 521–523.
[133] K. Kalyanasundaram, M. Neumann-Spallart, J. Phys. Chem. Lett. 86 (1982) 5163–5169.
[134] D. Wang, J.T. Groves, Proc. Natl. Acad. Sci. U. S. A. 110 (2013) 15579–15584.
[135] T. Nakazono, A.R. Parent, K. Sakai, Chem. Commun. 49 (2013) 6325–6327.
[136] T. Dhanasekaran, J. Grodkowski, P. Neta, P. Hambright, E. Fujita, J. Phys. Chem. A 103 (1999) 7742–7748.
[137] A.J. Morris, G.J. Meyer, E. Fujita, Acc. Chem. Res. 42 (2009) 1983–1994.
[138] C. Costentin, S. Drouet, M. Robert, J.-M. Savéant, J. Am. Chem. Soc. 134 (2012) 11235–11242.
[139] J.P. Collman, P.S. Wagenknecht, N.S. Lewis, J. Am. Chem. Soc. 114 (1992) 5665–5673.
[140] J.P. Collman, Y. Ha, P.S. Wagenknecht, M.A. Lopez, R. Guilard, J. Am. Chem. Soc. 115 (1993) 9080–9088.
[141] I. Bhugun, D. Lexa, J.-M. Savéant, J. Am. Chem. Soc. 118 (1996) 3982–3983.
[142] R.M. Kellett, T.G. Spiro, Inorg. Chem. 24 (1985) 2373–2377.
[143] T.-H. Chao, J.H. Espenson, J. Am. Chem. Soc. 100 (1978) 129–133.
[144] R.M. Kellett, T.G. Spiro, Inorg. Chem. 24 (1985) 2378–2382.
[145] C.H. Lee, D.K. Dogutan, D.G. Nocera, J. Am. Chem. Soc. 133 (2011) 8775–8777.
[146] M. Natali, A. Luisa, E. Iengo, F. Scandola, Chem. Commun. 50 (2014) 1842–1844.
[147] I. Aviv-Harel, Z. Gross, Coord. Chem. Rev. 255 (2011) 717–736.
[148] D.K. Dogutan, R. McGuire, D.G. Nocera, J. Am. Chem. Soc. 133 (2011) 9178–9180.
[149] H. Lei, A. Han, F. Li, M. Zhang, Y. Han, P. Du, W. Lai, R. Cao, Phys. Chem. Chem. Phys. 16 (2014) 1883–1893.
[150] B. Mondal, K. Sengupta, A. Rana, A. Mahammed, M. Botoshansky, S.G. Dey, Z. Gross, A. Dey, Inorg. Chem. 52 (2013) 3381–3387.
[151] A. Mahammed, B. Mondal, A. Rana, A. Dey, Z. Gross, Chem. Commun. 50 (2014) 2725–2727.
[152] V. Artero, M. Chavarot-Kerlidou, M. Fontecave (Eds.), Angew. Chem., Int. 50 (2011) 7238–7266.